Does increasing horizontal resolution improve the simulation of intense tropical rainfall?

Akshaya C Nikumbh[1], Pu Lin[2], David Paynter[3], and Yi Ming[4]

[1]Princeton Universitysity
[2]Princeton University
[3]GFDL/NOAA
[4]Boston College

October 17, 2023

Abstract

We examine tropical rainfall from Geophysical Fluid Dynamics Laboratory's Atmosphere Model version 4 (GFDL AM4) at three horizontal resolutions of 100 km, 50 km, and 25 km. The model produces more intense rainfall at finer resolutions, but a large discrepancy still exists between the simulated and the observed frequency distribution. We use a theoretical precipitation scaling diagnostic to examine the frequency distribution of the simulated rainfall. The scaling accurately produces the frequency distribution at moderate-to-high intensity ([?]10 mm day-1). Intense tropical rainfall at finer resolutions is produced primarily from the increased contribution of resolved precipitation and enhanced updrafts. The model becomes more sensitive to the grid-scale updrafts than local thermodynamics at high rain rates as the contribution from the resolved precipitation increases. On the contrary, the observed tropical precipitation extremes do not show a strong sensitivity to the grid-scale updrafts.

Does increasing horizontal resolution improve the simulation of intense tropical rainfall?

Akshaya C. Nikumbh[1,2], Pu Lin[1,2], David Paynter [2], Yi Ming[3]

[1] Atmospheric and Oceanic Sciences, Princeton University, Princeton, New Jersey
[2]Geophysical Fluid Dynamics Laboratory (NOAA), Princeton, New Jersey
[3]Schiller Institute for Integrated Science and Society, Boston College, Massachusetts

Key Points:

- Increasing horizontal resolution yields more intense tropical rainfall but not the accurate frequency distribution.
- Theoretical precipitation scaling accurately captures the frequency distribution of the simulated precipitation at moderate-to-high intensity
- Simulated precipitation extremes are more sensitive to the grid-scale updrafts than observed precipitation extremes

Corresponding author: Akshaya C. Nikumbh, akshaya.nikumbh@princeton.edu

Abstract

We examine tropical rainfall from Geophysical Fluid Dynamics Laboratory's Atmosphere Model version 4 (GFDL AM4) at three horizontal resolutions of 100 km, 50 km, and 25 km. The model produces more intense rainfall at finer resolutions, but a large discrepancy still exists between the simulated and the observed frequency distribution. We use a theoretical precipitation scaling diagnostic to examine the frequency distribution of the simulated rainfall. The scaling accurately produces the frequency distribution at moderate-to-high intensity ($\geq$10 $mm\ day^{-1}$). Intense tropical rainfall at finer resolutions is produced primarily from the increased contribution of resolved precipitation and enhanced updrafts. The model becomes more sensitive to the grid-scale updrafts than local thermodynamics at high rain rates as the contribution from the resolved precipitation increases. On the contrary, the observed tropical precipitation extremes do not show a strong sensitivity to the grid-scale updrafts.

Plain Language Summary

State of the art global scale climate models have horizontal resolutions of the order of tens of kilometers. However, these resolutions are much lower than the scales required to resolve tropical convection. This study investigates whether a resolution increase from 100 km to 25 km leads to any notable improvements in tropical rainfall simulation. Higher resolution simulations capture more intense rainfall events that are missed by their coarser counterparts. However, they struggle to capture the accurate frequency distribution of intense rainfall events. In addition, intense precipitation events in higher resolution simulations have different environmental conditions than the observed intense precipitation events. Results reported in this study underscore the importance of scrutinizing and carefully interpreting the outcomes of high-resolution climate model simulations.

1 Introduction

The representation of tropical rainfall is severely limited by the horizontal resolution of climate models, which is usually at the order of 100 km, whereas typical widths of upward motion in mature convective systems are in order of a few hundred meters to several kilometers (LeMone & Zipser, 1980; Matsuno, 2016). Convective systems interact with atmospheric circulation at various scales ranging from mesoscale to planetary-scale motions (Tomassini, 2020). Though many efforts have been made to count for the unresolved convection via the cumulus parameterization, these schemes are far from perfect and suffer large uncertainties. Therefore, increasing the resolution and improving cumulus parameterization remain the major focus areas of model development.

Though increasing horizontal resolution has model-dependent impacts, some common features are shared by a variety of general circulation models. They include increased contribution from the resolved precipitation, an intensified mean hydrological cycle and a higher frequency of precipitation extremes (Pope & Stratton, 2002; Demory et al., 2014; Hertwig et al., 2015; Terai et al., 2018; Herrington & Reed, 2020). Studies have also reported improved simulations of tropical and extratropical cyclones as the horizontal resolution increases (Zhao et al., 2009; Jung et al., 2012; Bacmeister et al., 2014; Demory et al., 2014). High-resolution ($\sim$50 km) versions of the Geophysical Fluid Dynamics Laboratory's (GFDL) gerneral circulation model have shown significant improvements in simulations of tropical cyclones, atmospheric rivers, mesoscale convective systems and precipitation extremes (Zhao et al., 2009; Murakami et al., 2020; Zhao, 2020, 2022; Dong et al., 2023; Jong et al., 2023).

Finer scales of resolved motions and a better representation of orography in high resolution simulations are recognized to improve the representation of precipitation extremes. Studies show that stronger vertical motions result in strengthening of precipitation (eg., Terai et al. (2018); Herrington and Reed (2020)). However, a recent study using aquaplanet simulations at resolutions ranging from 50 km to 6 km (Lin et al., 2022) show that increasing vertical motion do not fully explain the changes in precipitation intensity in high resolution simulations. Donner et al. (2016) highlight the need to assess the influence of vertical motions in examining the impacts of changing resolution and simulating convection in the models. Precipitation extremes over land, the global mean precipitation rates, their patterns and evaporation rate do not always show consistent improvement as the model resolution increases (Bador et al., 2020; Pope & Stratton, 2002; Hourdin et al., 2013; Bacmeister et al., 2014; Hertwig et al., 2015). Therefore, it is essential to develop a process-based understanding of how increasing resolution changes the simulation of rainfall. In the present work, we use GFDL's AM4 model to examine tropical rainfall distribution for three different resolutions viz., 100 km, 50 km and 25 km. We assess the frequency distribution of rainfall rates using the theoretical precipitation scaling diagnostic proposed by O'Gorman and Schneider (2009).

2 Data and methods

We use the GFDL atmospheric model version 4 (AM4) (Zhao et al., 2018a, 2018b) at three horizontal resolutions. The default GFDL AM4 utilizes a cubed-sphere topology for the atmospheric dynamical core with 96×96 grid boxes (c96) per cube face resulting in a horizontal resolution of ∼100 km. Here, we use two additional high resolution AM4 versions with 192×192 (c192) and 384×384 (c384) grid boxes per cube face, corresponding to horizontal resolutions of ∼50 km and ∼25 km, respectively. The default GFDL AM4.0 (Zhao et al., 2018a, 2018b) serves as the atmospheric component of GFDL's physical climate model (CM4, Held et al. (2019)), which participated in phase 6 of the Coupled Model Intercomparison Project (CMIP6, Eyring et al. (2016)). c192AM4 (Zhao, 2020) participated in the CMIP6 High Resolution Model Intercomparison Project (HighResMIP, Haarsma et al. (2016)). All three resolutions share the same atmospheric parameter setting as c192AM4 to remove uncertainties due to tuning. The parameter setting is documented in Zhao (2020). The default AM4 model's performance is reported in Zhao et al. (2018a) and Zhao et al. (2018b). The performance of c192AM4 in simulating the mean precipitation and precipitation extremes is documented in detail in Zhao (2020) and Zhao (2022).

The global mean precipitation in three different resolutions viz., c96, c192, and c384 are 2.92 $mm\ day^{-1}$, 2.96 $mm\ day^{-1}$, and 2.99$mm\ day^{-1}$, respectively for the period 1980-2000. The global mean precipitation increases progressively as the horizontal resolution of the model increases. Earlier studies (Duffy et al., 2003; Terai et al., 2018; Herrington & Reed, 2020) have noted a similar effect of horizontal resolution on simulated precipitation. These values are higher than the observed global mean precipitation of 2.67 $mm\ day^{-1}$ obtained using the the Global Precipitation Climatology Project (GPCP) dataset one degree daily dataset (1DD) Version 1.3 (Huffman et al., 2001) over the same period. Disagreement in the net longwave and shortwave fluxes at the surface (Supplementary Table 1) compared to observations (Trenberth et al., 2009) hint towards the differences in the mean simulated precipitation than the observed values. However, it is also important to note that the reliability of the GPCP dataset has been controversial (Gehne et al., 2016) and the radiative fluxes at the surface in the model lie within the range of different observational estimates (Trenberth et al., 2009; Stephens et al., 2012; Wild et al., 2015; L'Ecuyer et al., 2015). The excessive precipitation in the Western Pacific near the Philippines (also known as the "'Philippines hotspot" bias) and the dry biases over the eastern Atlantic and the Indian Ocean for c96 (Supplementary Fig. 1a) are reduced in c192 and c384 (Supplementary Fig. 1 b,c). However, the maritime continents (Supple-

mentary Fig. 1 b,c) and the eastern Pacific Inter Tropical Convergence Zone (ITCZ) move towards a wetter bias as the resolution increases. Tuning the model could improve some of the flux biases and thereby the mean precipitation biases. Zhao et al. (2018b) has investigated the effect of tuning on GFDL's AM4 precipitation in detail.

The model runs are analyzed for the historical period (1980-2000) at the daily frequency. We use daily precipitation dataset from the Tropical rainfall measurement mission (TRMM) version 3B42 (Huffman et al., 2007) and GPCP (Huffman et al., 2001) to compare the model performance with observations. The comparison of the model runs with observations are done for a common period of 1998-2000 over the tropics (30°S-30°N). In addition, we use the daily mean of the European Centre for Medium-Range Weather Forecasts (ECMWF) Reanalysis v5 (ERA5) (Hersbach et al., 2020) data at a horizontal resolution of $1^\circ \times 1^\circ$ for tropospheric temperature and winds. All model and observational variables are regridded to $1^\circ \times 1^\circ$ horizontal resolution using conservative remapping algorithm (python-cdo, (Schulzweida, 2022)). Histograms are normalized by a total number of data points that includes both rainy and non-rainy days.

3 Results

3.1 Rainfall intensity and frequency distribution

Figure 1 shows the normalized histogram of total daily precipitation intensity from the model at three resolutions (c96, c192, and c384) and observations (TRMM and GPCP). The normalized histogram (Fig. 1a) shows the most frequent nonzero rain rate. The simulated tropical rainfall peaks at ~ 1 $mm\ day^{-1}$. On the other hand, GPCP has a peak near $\sim$10-15 $mm\ day^{-1}$. All three resolutions produce more frequent rainfall than observations at lower rainrates (≤ 10 $mm\ day^{-1}$). This *too frequent too light* precipitation bias (also known as drizzle bias) is a shared problem in the most general circulation models (Sun et al., 2006; Wilcox & Donner, 2007; Stephens et al., 2010; Pendergrass & Hartmann, 2014). It is also important to note that the observations suffer from the underestimation of light rainfall (Behrangi et al., 2012). TRMM has a broad frequency distribution without any clear peak. Precipitation radar aboard TRMM has a minimum detectable signal of 17 dBz, making it poorly suited for detection of light rainfall (Behrangi et al., 2012; Kummerow et al., 1998). The discrepancy in the frequency of light rainfall is therefore partly attributed to the observational uncertainty.

The impact of horizontal resolution is evident at moderate rainfall rates. Interestingly, c384 has a notable reduction in the frequency near the secondary peak for c96 and c192 ($\sim 3-10$ $mm\ day^{-1}$). The bimodal frequency distribution of rainfall in c96 and c192 becomes monomodal in c384. The removal of a secondary peak in c384 is mainly due to the reduction in parameterized rainfall in c384 at these rainrates (Fig. 1c). All three resolutions produce less frequent rainfall at moderate rainfall rates ($20-40$ $mm\ day^{-1}$) compared to observations. On the contrary, the frequency of heavy rainfall ($\geq$ 100 $mm\ day^{-1}$) is overestimated compared to GPCP in all three resolutions. The frequency of high precipitation events in the model is closer to TRMM than GPCP. The retrieved precipitation in TRMM is shown to be more reliable than GPCP at higher rain rates (Behrangi et al., 2012). The frequency of heavy rainfall in c384 and c192 is overestimated compared to TRMM, whereas it is underestimated in c96.

The normalized histogram with a linear rainfall intensity scale (Fig. 1b) highlights the upper tail of rainfall distribution. The model produces progressively more frequent high rainfall events as the resolution increases. A few rare events with very high intensity (≥ 300 $mm\ day^{-1}$) are captured by c384 and c192 but not by c96. The observed precipitation tail goes up to 1000 $mm\ day^{-1}$, which is not captured by either resolution. On the contrary, it is also important to note that the frequency of high precipitation events ($\sim$200-400 $mm\ day^{-1}$) is overestimated in high resolution simulations (c192 and c384)

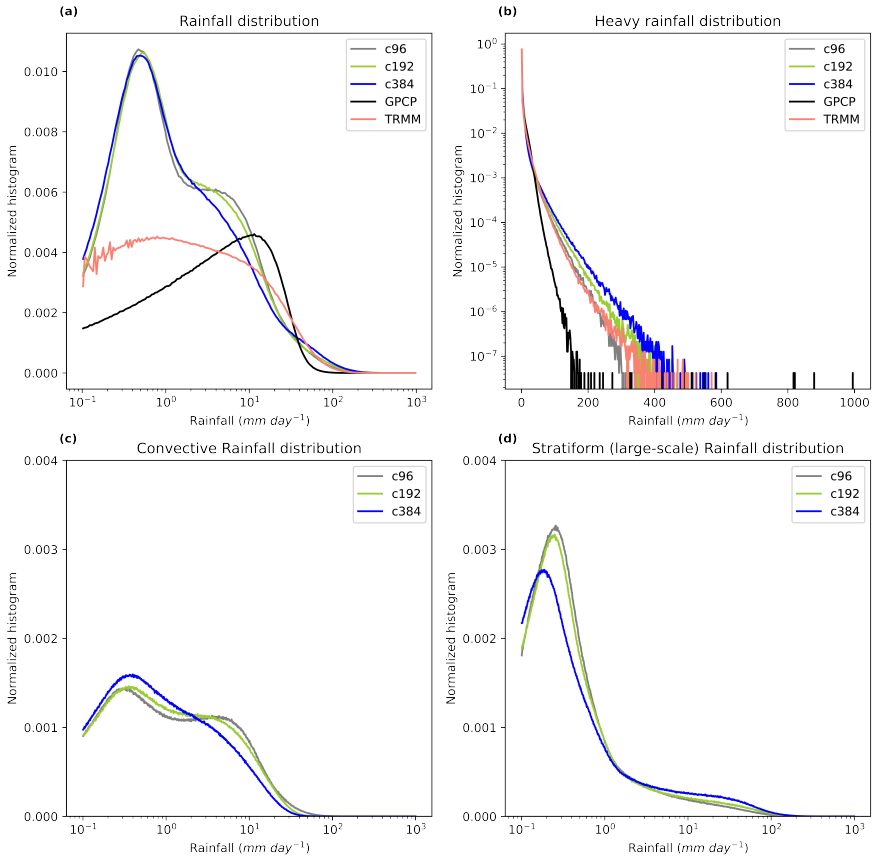

Figure 1. Normalized histogram of the daily mean rainfall (a) over logarithmic-scaled bins (rainfall intensity in $mm\ day^{-1}$), (b) over a linear-scaled bins (rainfall intensity) and a logarithmic scale for y-axis (normalized histogram) to highlight the upper end of the distribution. Normalized histogram for (c) convective rainfall, (d) resolved/large-scale rainfall. The simulated (c96, c192, c384) and observed (TRMM and GPCP) precipitation datasets are regridded to $1°\times1°$ horizontal resolution using conservative remapping algorithm. Histograms are normalized by a total count of datapoints considering both rainy and nonrainy days. The figure is plotted for an overlap period of 1998-2000 for the model runs and observations over the tropics (30°S-30°N).

compared to the observations. This analysis shows that the model produces intense tropical rainfall with the increasing horizontal resolution, but it overestimates the frequency of precipitation extremes.

3.2 Factors affecting the rainfall intensity distribution

Increasing the horizontal resolution changes the partitioning between precipitation produced by the convection scheme (parameterized precipitation, *prec_conv*) and the large-scale scheme (resolved precipitation, *prec_ls*). The contribution of resolved precipitation to the mean precipitation in the tropics increases from about 30% in c96 to more than 50% in c384 (Supplementary Fig. 2). The normalized frequency distribution for convective rainfall shifts towards lower intensity as the horizontal resolution increases (Fig. 1c). It is indicated by a progressively higher peak of normalized histogram at low convective

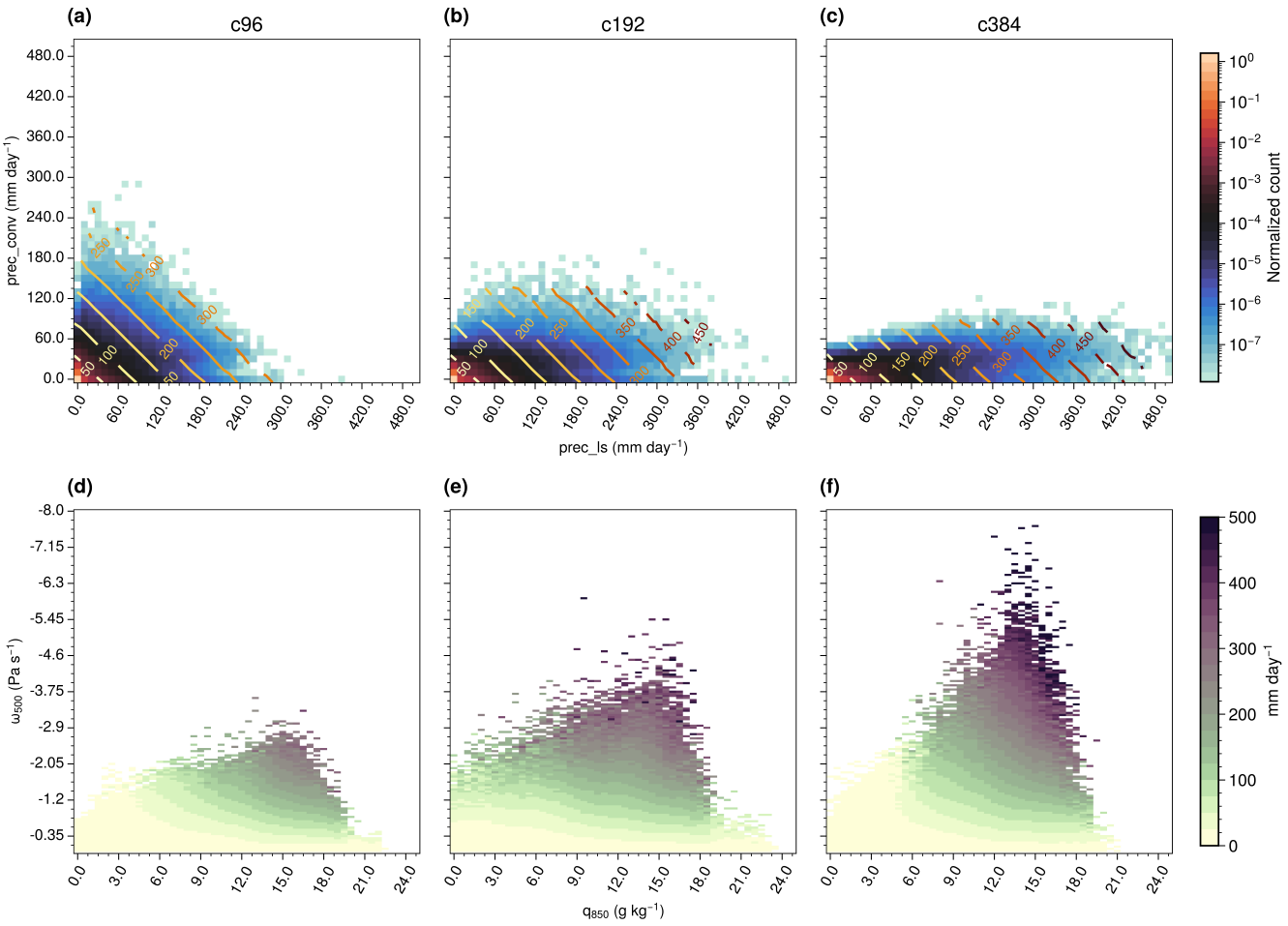

Figure 2. (a) 2D bin mean of normalized count (shading) and mean precipitation intensity (in $mm\ day^{-1}$ indicated by contours) as a function of convective (prec_conv) and large-scale (prec_ls) rainfall. (b) 2D bin mean precipitation intensity ($mm\ day^{-1}$) as a function of low-level moisture (q_{850}) and mid-tropospheric pressure velocity (ω_{500}). The figure is plotted for model simulations over a historical period of 1980-2000.

rainfall rates ($\leq$2 $mm\ day^{-1}$) and a reduction in the frequency at higher rainrates as the horizontal resolution increases (Fig. 1c). On the other hand, the frequency of large-scale rainfall exhibit a reduction in the peak at low rainfall rates and an increase at high rain rates for high resolution runs (Fig. 1d). This shows that the large-scale scheme progressively does more work at high rainfall intensities as the horizontal resolution increases. Figure 2 a-c shows the joint distribution of the resolved and the parameterized precipitation. The shading represents the 2D bin mean normalized count and the contours show the mean precipitation intensity. The count is normalized by a total number of datapoints considering both rainy and non-rainy days. For c96, both parameterized and large-scale schemes contribute almost equally at all precipitation intensities. However, the partitioning between parameterized and resolved precipitation changes in c192 and c384. Intense rainfall in c192 and c384 comes mainly from the large-scale scheme. Convective rainfall in c96 contributes up to a maximum intensity of 300 $mm\ day^{-1}$. However, it de-

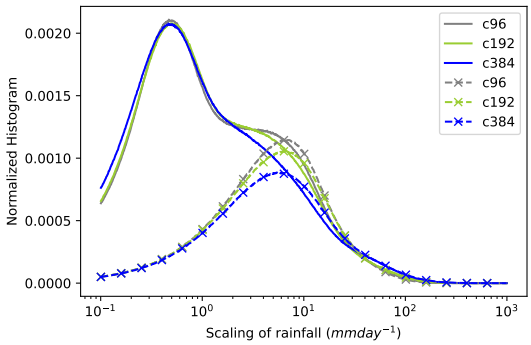

Figure 3. Normalized histogram of the model simulated mean daily rainfall (solid lines) and rainfall obtained from the theoretical precipitation scaling (marked-dotted lines) using equation (1). The histograms are plotted for the model runs over a historical period of 1980-2000.

creases below 200 $mm\ day^{-1}$ in c192 and it decreases even further in c384 (below 120 $mm\ day^{-1}$).

Two important ingredients to understand the rainfall intensity distribution are moisture and updraft velocity. We look at the 2D distribution of precipitation intensity as a function of low level moisture (q_{850}) and mid-tropospheric updraft velocity (ω_{500}) for three different resolutions (Fig. 2). As expected, rainfall intensity increases as moisture content and vertical velocity increase. The range of moisture content in three resolutions is not much different, however, the maximum vertical velocity increases by a factor of ~ 1.7 from c96 to c192, and about $\sim$2.3 from c96 to c384. Intense rainfall at finer resolutions mainly occurs at high updraft velocity (Fig. 2 e, f). In addition, the sensitivity of the precipitation intensity to high updraft velocity is contributed mainly by the resolved precipitation (Supplementary Fig. 3). In all three resolutions, large-scale precipitation shows a more sensitivity to updrafts than moisture (Supplementary Fig. 3 d-f). The parameterized precipitation instead shows sensitivity to low-level moisture unlike the resolved precipitation (Supplementary Fig. 3 a-c). Qualitative similarities between the total rainfall intensity distribution (Fig. 2 d-f) and the resolved precipitation (Supplementary Fig. 3 d-f) suggests that the sensitivity of precipitation intensity to the updraft velocity at high rainrates comes primarily from the resolved precipitation. This analysis indicates that as the horizontal resolution increases, the increase in rainfall intensity is associated primarily with the enhanced updraft velocity rather than the moisture content, and these changes come mainly from resolved (large-scale) precipitation.

3.3 Precipitation scaling

To further understand the impact of horizontal resolution on the rainfall frequency distribution, we use the precipitation scaling diagnostic proposed by O'Gorman and Schneider (2009). This diagnostic has been used primarily to study the changes in precipitation extremes with warming (O'Gorman, 2012; Singh & O'Gorman, 2014; Pfahl et al., 2017; Nie et al., 2018). The scaling is given by

$$P \approx -\left\{\omega \frac{\partial q_s}{\partial p}|_{\theta^*}\right\} \tag{1}$$

where precipitation intensity (P) is calculated from a column integrated product of pressure velocity (ω) and the vertical derivative of saturation specific humidity taken along a moist adiabat profile($\frac{\partial q_s}{\partial p}|_{\theta^*}$). The right hand side of the equation (1) corresponds to the column integrated condensation rate. The condensation maintains saturation of the

rising air parcel. This scaling assumes that precipitation efficiency is ~ 1 and all of the condensed water vapor falls as rainfall. The diabatic effects other than latent heating are neglected (θ^* is conserved; shown by Muller et al. (2011)). This scaling is expected to work better at higher precipitation intensities when air parcels are nearly saturated. However, we test it at all intensities.

The scaling captures the spatial distribution of deep convective areas of the tropics quite well, but it underestimates the intensity of the mean rainfall (Supplementary Fig. 4). Despite the assumptions mentioned earlier, the scaling captures the frequency distribution of rainfall at moderate to high intensity remarkably well in all three resolutions (Fig. 3 a). The scaling does not capture the model drizzle. We will discuss the possible reasons for it shortly. The frequency distribution of rainfall obtained by the scaling is monomodal. It peaks near 5-8 $mm\ day^{-1}$ for all three resolutions, which is close to the secondary peak of rainfall frequency distribution in c96 and c192. The scaling accurately produces this peak and captures the increasing magnitude from c384 to c96. After this peak, the precipitation scaling closely follows the frequency of simulated precipitation in all three resolutions. At moderate and high rainfall intensities, it overestimates the frequency of model simulated precipitation. However, the scaling captures the overall shape at high rain rates, including a peak in c384 near 50 $mm\ day^{-1}$.

As the contribution from radiative fluxes other than latent heat is non-negligible (θ^* is not conserved) at low rainfall intensity, the scaling is not expected to work at low rain rates. In addition, the model drizzle mainly comes from the subsaturated regions ($q \ll q_s$) (Terai et al., 2016). Earlier work suggests that a crude representation of parameterized convection could be the cause of drizzle bias in the models (Suzuki et al., 2013; Stephens et al., 2010). As we use grid-scale (resolved) variables to estimate the precipitation scaling, it can not capture subgrid scale convective processes. The above reasons possibly explain why precipitation scaling does not reproduce an accurate frequency of the model drizzle. In addition, the above scaling formulation does not include precipitation efficiency. The large-scale precipitation efficiency is affected by several factors such as mid level moisture, Convective available potential energy (CAPE), convective organization and microphysical processes (Muller & Takayabu, 2020; Zhao et al., 2016; Singh & O'Gorman, 2014). The overestimation of high rain rates by the scaling is likely due to the omission of precipitation efficiency in the calculations.

We plot the 2D bin mean of normalized precipitation intensity as a function of column-integrated vertical velocity ($\{\omega\}$) and the column-integrated vertical derivative of saturated specific humidity ($\left\{\frac{\partial q_s}{\partial p}|_{\theta*}\right\}$) (Fig. 4). As the maximum precipitation intensity in simulations and observations vary over a large range (Fig. 1 b), we normalize precipitation intensity by the maximum 2D bin mean value for each dataset. The precipitation intensity distribution without normalizing has similar features (Supplementary Fig. 5). The increase in precipitation intensity at higher resolution comes mainly from the changes in updraft velocity rather than changes in thermal stratification ($\left\{\frac{\partial q_s}{\partial p}|_{\theta*}\right\}$) as the horizontal resolution increases (Fig. 4 a-c). Intense precipitation events in the model are strongly tied to the grid-scale updrafts unlike observations (Fig. 4 e-f). We see that observed heavy precipitation events can occur even at moderate updrafts if the thermal stratification (Fig. 4 e-f, Supplementary Fig. 5 e-f) or low-level moisture (Supplementary Fig. 6 e-f) is high. Interestingly, ERA5 precipitation is also tied to stronger grid-scale updrafts but relatively to a lesser extent than GFDL's AM4 model. In c384, the grid-scale updrafts are much more intense than the reanalysis updrafts. The maximum grid-scale updraft at 500 hPa in c384 is about two times the maximum grid-scale updraft in ERA5 (Supplementary Fig. 6). It should be noted that the updrafts in reanalysis datasets suffer from uncertainties (Uma et al., 2021). Nonetheless, observational studies have noted the importance of local thermodynamics for tropical rainfall and the onset of precipitation (Houze Jr, 1989; Bretherton et al., 2004; Neelin et al., 2022). A typical size of updrafts in tropical convective systems is in order of a few kilometers (LeMone & Zipser,

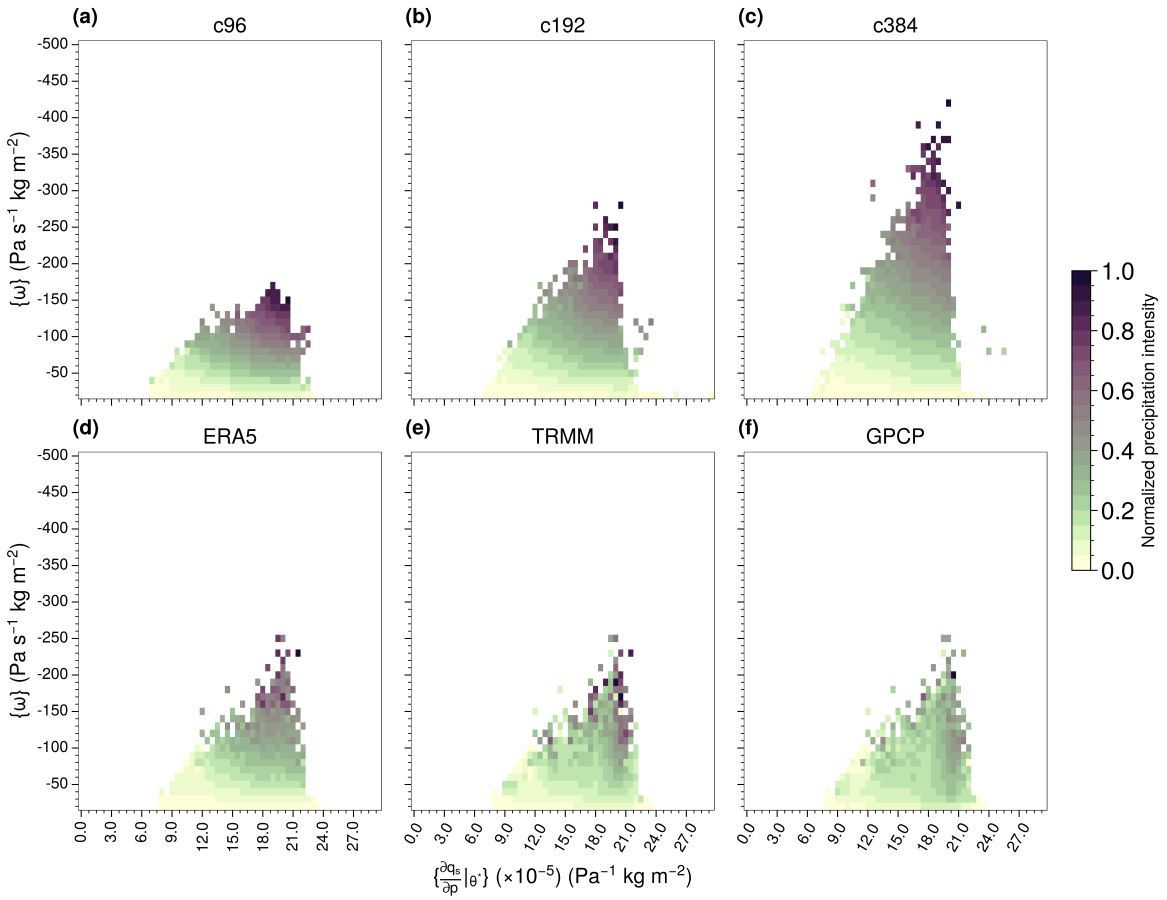

Figure 4. 2D bin mean of normalized precipitation intensity as a function of column-integrated pressure velocity $\{\omega\}$ and the column-integrated vertical derivative of saturated specific humidity along the moist adiabat $\left\{\frac{\partial q_s}{\partial p}|_{\theta*}\right\}$. Precipitation intensity (in $mm\ day^{-1}$) is normalized by maximum 2D bin value for each subplot. The figure is plotted using the data for an overlap period of 1998-2000.

1980; Matsuno, 2016), we would expect the cancellation of updrafts and downdrafts when averaged over an area of $\sim 1°\times1°$. In turn, we expect to see a less dependence of grid-scale updrafts for observed precipitation extremes.

Intense precipitation in c384 and c192 are closely tied to strong updrafts. The sensitivity of the simulated precipitation to the grid-scale updraft velocity mainly comes from the resolved precipitation and not from the parameterized precipitation (Supplementary Fig. 3). In this regard, tropical precipitation extremes in high resolution simulations exhibit similarities to grid-scale storms (Held et al., 2007). This suggests that even though the model is able to capture high intensity events as the horizontal resolution increases, with the increased contribution from the resolved precipitation, it comes at the expense of the model being overly sensitive to the grid-scale updraft velocity.

4 Discussion

We examine the distribution of tropical rainfall using GFDL's AM4 model at three horizontal resolutions viz., c96 (∼100 km), c192 (∼50 km) and c384 (∼25 km). As the horizontal resolution increases, we observe a progressive increase in the upper percentile of rainfall (precipitation extremes), increased contribution from the resolved precipitation and enhanced vertical velocities. These features are similar to earlier studies using different general circulation models (eg., Terai et al. (2018); Herrington and Reed (2020)). The model overestimates the frequency of light rainfall (drizzle bias) and underestimates the moderate rainfall in all three simulations. At finer resolutions (c192 and c384), the model produces more intense rainfall, but it overestimates the frequency of occurrence of heavy rainfall events compared to observed datasets (Fig. 1). The increase in precipitation extremes at high resolution is primarily contributed by the resolved precipitation and mainly comes from enhanced updrafts (Fig. 2).

We use theoretical precipitation scaling proposed by O'Gorman and Schneider (2009) to assess the frequency distribution of tropical rainfall. The scaling utilizes the grid-scale vertical velocity and temperature profiles to estimate an approximate precipitation intensity. Despite this simple formulation, the scaling produces the frequency distribution of model simulated precipitation remarkably well at moderate to high rain rates (Figure 3). Earlier studies have used the scaling to examine changes in precipitation extremes (O'Gorman, 2012; Singh & O'Gorman, 2014; Pfahl et al., 2017; Nie et al., 2018). In the GFDL model, the scaling reproduces the frequency distribution of tropical rainfall even at moderate rainfall rates ($\geq 10\ mm\ day^{-1}$). This could be a model dependent result, but it would be interesting to check the scaling for the other general circulation models.

Precipitation extremes in the model are closely tied to the grid-scale intense updrafts and relatively less sensitive to thermal stratification (Figure 4 a-c) and low-level moisture (Supplementary Fig. 6 a-c). In observed datasets, however, intense precipitation events can occur at moderate updraft velocities if thermal stratification (Figure 4 e-f) and low-level moisture are high (Supplementary Fig. 6 e-f). This high sensitivity of the model to updrafts comes mainly from the resolved precipitation (Supplementary Fig. 3). Convective precipitation shows sensitivity to local thermodynamics mimicking the observed tropical precipitation behavior closely (Bretherton et al., 2004; Neelin et al., 2022). On the other hand, resolved precipitation has been shown to capture geographical patterns and rain rates (Kooperman et al., 2018) better than parameterized precipitation. Convective precipitation also struggles to capture the accurate diurnal cycle of precipitation (Zhao et al., 2018a). This study suggests that the amount of rainfall obtained from the resolved precipitation and its sensitivity to the grid-scale vertical motion should be examined carefully atleast until the updrafts and downdrafts in convective systems are resolved explicitly. We reiterate the suggestion by Donner et al. (2016) on the importance of recognizing the dependence of resolved vertical velocity on resolution and utilizing it to understand the impacts of resolution realistically. Our results suggest that additional process-based evaluation is necessary to assess the performance of both parameterized and resolved precipitation.

References

Bacmeister, J. T., Wehner, M. F., Neale, R. B., Gettelman, A., Hannay, C., Lauritzen, P. H., ... Truesdale, J. E. (2014). Exploratory high-resolution climate simulations using the community atmosphere model (cam). *Journal of Climate*, *27*(9), 3073–3099.

Bador, M., Boé, J., Terray, L., Alexander, L. V., Baker, A., Bellucci, A., ... others (2020). Impact of higher spatial atmospheric resolution on precipitation extremes over land in global climate models. *Journal of Geophysical Research:*

Atmospheres, *125*(13), e2019JD032184.

Behrangi, A., Lebsock, M., Wong, S., & Lambrigtsen, B. (2012). On the quantification of oceanic rainfall using spaceborne sensors. *Journal of Geophysical Research: Atmospheres*, *117*(D20).

Bretherton, C. S., Peters, M. E., & Back, L. E. (2004). Relationships between water vapor path and precipitation over the tropical oceans. *Journal of climate*, *17*(7), 1517–1528.

Demory, M.-E., Vidale, P. L., Roberts, M. J., Berrisford, P., Strachan, J., Schiemann, R., & Mizielinski, M. S. (2014). The role of horizontal resolution in simulating drivers of the global hydrological cycle. *Climate dynamics*, *42*, 2201–2225.

Dong, W., Zhao, M., Ming, Y., Krasting, J. P., & Ramaswamy, V. (2023). Simulation of united states mesoscale convective systems using gfdl's new high-resolution general circulation model. *Journal of Climate*, 1–40.

Donner, L. J., O'Brien, T. A., Rieger, D., Vogel, B., & Cooke, W. F. (2016). Are atmospheric updrafts a key to unlocking climate forcing and sensitivity? *Atmospheric Chemistry and Physics*, *16*(20), 12983–12992.

Duffy, P., Govindasamy, B., Iorio, J., Milovich, J., Sperber, K., Taylor, K., ... Thompson, S. (2003). High-resolution simulations of global climate, part 1: present climate. *Climate Dynamics*, *21*, 371–390.

Eyring, V., Bony, S., Meehl, G. A., Senior, C. A., Stevens, B., Stouffer, R. J., & Taylor, K. E. (2016). Overview of the coupled model intercomparison project phase 6 (cmip6) experimental design and organization. *Geoscientific Model Development*, *9*(5), 1937–1958.

Gehne, M., Hamill, T. M., Kiladis, G. N., & Trenberth, K. E. (2016). Comparison of global precipitation estimates across a range of temporal and spatial scales. *Journal of Climate*, *29*(21), 7773–7795.

Haarsma, R. J., Roberts, M. J., Vidale, P. L., Senior, C. A., Bellucci, A., Bao, Q., ... others (2016). High resolution model intercomparison project (highresmip v1. 0) for cmip6. *Geoscientific Model Development*, *9*(11), 4185–4208.

Held, I. M., Guo, H., Adcroft, A., Dunne, J., Horowitz, L., Krasting, J., ... others (2019). Structure and performance of gfdl's cm4. 0 climate model. *Journal of Advances in Modeling Earth Systems*, *11*(11), 3691–3727.

Held, I. M., Zhao, M., & Wyman, B. (2007). Dynamic radiative–convective equilibria using gcm column physics. *Journal of the atmospheric sciences*, *64*(1), 228–238.

Herrington, A. R., & Reed, K. A. (2020). On resolution sensitivity in the community atmosphere model. *Quarterly Journal of the Royal Meteorological Society*, *146*(733), 3789–3807.

Hersbach, H., Bell, B., Berrisford, P., Hirahara, S., Horányi, A., Muñoz-Sabater, J., ... others (2020). The era5 global reanalysis. *Quarterly Journal of the Royal Meteorological Society*, *146*(730), 1999–2049.

Hertwig, E., von Storch, J.-S., Handorf, D., Dethloff, K., Fast, I., & Krismer, T. (2015). Effect of horizontal resolution on echam6-amip performance. *Climate Dynamics*, *45*, 185–211.

Hourdin, F., Foujols, M.-A., Codron, F., Guemas, V., Dufresne, J.-L., Bony, S., ... others (2013). Impact of the lmdz atmospheric grid configuration on the climate and sensitivity of the ipsl-cm5a coupled model. *Climate Dynamics*, *40*, 2167–2192.

Houze Jr, R. A. (1989). Observed structure of mesoscale convective systems and implications for large-scale heating. *Quarterly Journal of the Royal Meteorological Society*, *115*(487), 425–461.

Huffman, G. J., Adler, R. F., Morrissey, M. M., Bolvin, D. T., Curtis, S., Joyce, R., ... Susskind, J. (2001). Global precipitation at one-degree daily resolution from multisatellite observations. *Journal of hydrometeorology*, *2*(1), 36–50.

Huffman, G. J., Bolvin, D. T., Nelkin, E. J., Wolff, D. B., Adler, R. F., Gu, G., ... Stocker, E. F. (2007). The trmm multisatellite precipitation analysis (tmpa): Quasi-global, multiyear, combined-sensor precipitation estimates at fine scales. *Journal of hydrometeorology*, *8*(1), 38–55.

Jong, B.-T., Delworth, T. L., Cooke, W. F., Tseng, K.-C., & Murakami, H. (2023). Increases in extreme precipitation over the northeast united states using high-resolution climate model simulations. *npj Climate and Atmospheric Science*, *6*(1), 18.

Jung, T., Miller, M., Palmer, T., Towers, P., Wedi, N., Achuthavarier, D., ... others (2012). High-resolution global climate simulations with the ecmwf model in project athena: Experimental design, model climate, and seasonal forecast skill. *Journal of Climate*, *25*(9), 3155–3172.

Kooperman, G. J., Pritchard, M. S., O'Brien, T. A., & Timmermans, B. W. (2018). Rainfall from resolved rather than parameterized processes better represents the present-day and climate change response of moderate rates in the community atmosphere model. *Journal of advances in modeling earth systems*, *10*(4), 971–988.

Kummerow, C., Barnes, W., Kozu, T., Shiue, J., & Simpson, J. (1998). The tropical rainfall measuring mission (trmm) sensor package. *Journal of atmospheric and oceanic technology*, *15*(3), 809–817.

LeMone, M. A., & Zipser, E. J. (1980). Cumulonimbus vertical velocity events in gate. part i: Diameter, intensity and mass flux. *Journal of the Atmospheric Sciences*, *37*(11), 2444–2457.

Lin, P., Ming, Y., & Robinson, T. (2022). On the resolution sensitivity in a gfdl global atmospheric model. *Authorea Preprints*.

L'Ecuyer, T. S., Beaudoing, H., Rodell, M., Olson, W., Lin, B., Kato, S., ... others (2015). The observed state of the energy budget in the early twenty-first century. *Journal of Climate*, *28*(21), 8319–8346.

Matsuno, T. (2016). Prologue: tropical meteorology 1960–2010—personal recollections. *Meteorological Monographs*, *56*, vii–xv.

Muller, C., O'Gorman, P. A., & Back, L. E. (2011). Intensification of precipitation extremes with warming in a cloud-resolving model. *Journal of Climate*, *24*(11), 2784–2800.

Muller, C., & Takayabu, Y. (2020). Response of precipitation extremes to warming: what have we learned from theory and idealized cloud-resolving simulations, and what remains to be learned? *Environmental Research Letters*, *15*(3), 035001.

Murakami, H., Delworth, T. L., Cooke, W. F., Zhao, M., Xiang, B., & Hsu, P.-C. (2020). Detected climatic change in global distribution of tropical cyclones. *Proceedings of the National Academy of Sciences*, *117*(20), 10706–10714.

Neelin, J. D., Martinez-Villalobos, C., Stechmann, S. N., Ahmed, F., Chen, G., Norris, J. M., ... Lenderink, G. (2022). Precipitation extremes and water vapor: Relationships in current climate and implications for climate change. *Current Climate Change Reports*, *8*(1), 17–33.

Nie, J., Sobel, A. H., Shaevitz, D. A., & Wang, S. (2018). Dynamic amplification of extreme precipitation sensitivity. *Proceedings of the National Academy of Sciences*, *115*(38), 9467–9472.

Nikumbh, A., Lin, P., Paynter, D., & Ming, Y. (2023a, October). *Supporting data 1 for "Does increasing horizontal resolution improve the simulation of intense tropical rainfall?".* Zenodo. Retrieved from `https://doi.org/10.5281/zenodo.8433128` doi: 10.5281/zenodo.8433128

Nikumbh, A., Lin, P., Paynter, D., & Ming, Y. (2023b, October). *Supporting data 2 for "Does increasing horizontal resolution improve the simulation of intense tropical rainfall?".* Zenodo. Retrieved from `https://doi.org/10.5281/zenodo.8433235` doi: 10.5281/zenodo.8433235

Nikumbh, A., Lin, P., Paynter, D., & Ming, Y. (2023c, October). *Supporting data 3 for "Does increasing horizontal resolution improve the simulation of intense tropical rainfall?".* Zenodo. Retrieved from `https://doi.org/10.5281/zenodo.8433237` doi: 10.5281/zenodo.8433237

O'Gorman, P. A. (2012). Sensitivity of tropical precipitation extremes to climate change. *Nature Geoscience*, *5*(10), 697–700.

O'Gorman, P. A., & Schneider, T. (2009). Scaling of precipitation extremes over a wide range of climates simulated with an idealized gcm. *Journal of Climate*, *22*(21), 5676–5685.

Pendergrass, A. G., & Hartmann, D. L. (2014). Changes in the distribution of rain frequency and intensity in response to global warming. *Journal of Climate*, *27*(22), 8372–8383.

Pfahl, S., O'Gorman, P. A., & Fischer, E. M. (2017). Understanding the regional pattern of projected future changes in extreme precipitation. *Nature Climate Change*, *7*(6), 423–427.

Pope, V., & Stratton, R. (2002). The processes governing horizontal resolution sensitivity in a climate model. *Climate Dynamics*, *19*, 211–236.

Schulzweida, U. (2022, October). *Cdo user guide.* Zenodo. Retrieved from `https://doi.org/10.5281/zenodo.7112925` doi: 10.5281/zenodo.7112925

Singh, M. S., & O'Gorman, P. A. (2014). Influence of microphysics on the scaling of precipitation extremes with temperature. *Geophysical Research Letters*, *41*(16), 6037–6044.

Stephens, G. L., L'Ecuyer, T., Forbes, R., Gettelmen, A., Golaz, J.-C., Bodas-Salcedo, A., ... Haynes, J. (2010). Dreary state of precipitation in global models. *Journal of Geophysical Research: Atmospheres*, *115*(D24).

Stephens, G. L., Li, J., Wild, M., Clayson, C. A., Loeb, N., Kato, S., ... Andrews, T. (2012). An update on earth's energy balance in light of the latest global observations. *Nature Geoscience*, *5*(10), 691–696.

Sun, Y., Solomon, S., Dai, A., & Portmann, R. W. (2006). How often does it rain? *Journal of climate*, *19*(6), 916–934.

Suzuki, K., Golaz, J.-C., & Stephens, G. L. (2013). Evaluating cloud tuning in a climate model with satellite observations. *Geophysical Research Letters*, *40*(16), 4464–4468.

Terai, C. R., Caldwell, P., & Klein, S. A. (2016). Why do climate models drizzle too much and what impact does this have. In *Agu fall meeting abstracts* (Vol. 2016, pp. A53K–01).

Terai, C. R., Caldwell, P. M., Klein, S. A., Tang, Q., & Branstetter, M. L. (2018). The atmospheric hydrologic cycle in the acme v0. 3 model. *Climate Dynamics*, *50*(9-10), 3251–3279.

Tomassini, L. (2020). The interaction between moist convection and the atmospheric circulation in the tropics. *Bulletin of the American Meteorological Society*, *101*(8), E1378–E1396.

Trenberth, K. E., Fasullo, J. T., & Kiehl, J. (2009). Earth's global energy budget. *Bulletin of the american meteorological society*, *90*(3), 311–324.

Uma, K. N., Das, S. S., Ratnam, M. V., & Suneeth, K. V. (2021). Assessment of vertical air motion among reanalyses and qualitative comparison with very-high-frequency radar measurements over two tropical stations. *Atmospheric Chemistry and Physics*, *21*(3), 2083–2103.

Wilcox, E. M., & Donner, L. J. (2007). The frequency of extreme rain events in satellite rain-rate estimates and an atmospheric general circulation model. *Journal of Climate*, *20*(1), 53–69.

Wild, M., Folini, D., Hakuba, M. Z., Schär, C., Seneviratne, S. I., Kato, S., ... König-Langlo, G. (2015). The energy balance over land and oceans: an assessment based on direct observations and cmip5 climate models. *Climate Dynamics*, *44*, 3393–3429.

Zhao, M. (2020). Simulations of atmospheric rivers, their variability, and response to global warming using gfdl's new high-resolution general circulation model. *Journal of Climate*, *33*(23), 10287–10303.

Zhao, M. (2022). A study of ar-, ts-, and mcs-associated precipitation and extreme precipitation in present and warmer climates. *Journal of Climate*, *35*(2), 479–497.

Zhao, M., Golaz, J.-C., Held, I., Guo, H., Balaji, V., Benson, R., ... others (2018a). The gfdl global atmosphere and land model am4. 0/lm4. 0: 1. simulation characteristics with prescribed ssts. *Journal of Advances in Modeling Earth Systems*, *10*(3), 691–734.

Zhao, M., Golaz, J.-C., Held, I., Guo, H., Balaji, V., Benson, R., ... others (2018b). The gfdl global atmosphere and land model am4. 0/lm4. 0: 2. model description, sensitivity studies, and tuning strategies. *Journal of Advances in Modeling Earth Systems*, *10*(3), 735–769.

Zhao, M., Golaz, J.-C., Held, I. M., Ramaswamy, V., Lin, S.-J., Ming, Y., ... others (2016). Uncertainty in model climate sensitivity traced to representations of cumulus precipitation microphysics. *Journal of Climate*, *29*(2), 543–560.

Zhao, M., Held, I. M., Lin, S.-J., & Vecchi, G. A. (2009). Simulations of global hurricane climatology, interannual variability, and response to global warming using a 50-km resolution gcm. *Journal of Climate*, *22*(24), 6653–6678.

Open Research Section

The AM4 model code is provided at `https://data1.gfdl.noaa.gov/nomads/forms/am4.0/` (Zhao et al., 2018a, 2018b). The configuration of the simulations presented in this manuscript is described in Zhao (2020). The model outputs used are available at: `https://zenodo.org/record/8433128`, `https://zenodo.org/record/8433235` and `https://zenodo.org/record/8433237` (Nikumbh et al., 2023a, 2023b, 2023c). The ERA5 data can be downloaded from `https://cds.climate.copernicus.eu/cdsapp#!/dataset/reanalysis-era5-complete?tab=overview` (Hersbach et al., 2020). The GPCP precipitation dataset is available `https://rda.ucar.edu/datasets/ds728.7/dataaccess/` (Huffman et al., 2001). The TRMM precipitation data is downloaded from `https://disc.gsfc.nasa.gov/datasets?keywords=TRMM_3B42_7&page=1` (Huffman et al., 2007).

Acknowledgments

A.C.N. acknowledges support from Cooperative Institute for Modeling the Earth System, AOS, Princeton University, and Geophysical Fluid Dynamics Laboratory (GFDL), NOAA. The initial version of the manuscript greatly benefited from discussions and inputs from Dr. Leo Donner and Dr. Bor-Ting Jong. We thank Dr. Yi-Huang Kuo and Dr. Issac Held for discussions, Dr. Ming Zhao, Dr. Wenhao Dong and Dr. Huan Gao for helping to set up the initial model runs. This work was done by A.C.N. under Award NA18OAR4320123 from the National Oceanic and Atmospheric Administration, U.S. Department of Commerce. The statements, findings, conclusions, and recommendations are those of the author(s) and do not necessarily reflect the views of the National Oceanic and Atmospheric Administration or the U.S. Department of Commerce.

Does increasing horizontal resolution improve the simulation of intense tropical rainfall?

Akshaya C. Nikumbh[1,2], Pu Lin[1,2], David Paynter [2], Yi Ming[3]

[1] Atmospheric and Oceanic Sciences, Princeton University, Princeton, New Jersey
[2]Geophysical Fluid Dynamics Laboratory (NOAA), Princeton, New Jersey
[3]Schiller Institute for Integrated Science and Society, Boston College, Massachusetts

Key Points:

- Increasing horizontal resolution yields more intense tropical rainfall but not the accurate frequency distribution.
- Theoretical precipitation scaling accurately captures the frequency distribution of the simulated precipitation at moderate-to-high intensity
- Simulated precipitation extremes are more sensitive to the grid-scale updrafts than observed precipitation extremes

Corresponding author: Akshaya C. Nikumbh, akshaya.nikumbh@princeton.edu

Abstract

We examine tropical rainfall from Geophysical Fluid Dynamics Laboratory's Atmosphere Model version 4 (GFDL AM4) at three horizontal resolutions of 100 km, 50 km, and 25 km. The model produces more intense rainfall at finer resolutions, but a large discrepancy still exists between the simulated and the observed frequency distribution. We use a theoretical precipitation scaling diagnostic to examine the frequency distribution of the simulated rainfall. The scaling accurately produces the frequency distribution at moderate-to-high intensity ($\geq$10 $mm\ day^{-1}$). Intense tropical rainfall at finer resolutions is produced primarily from the increased contribution of resolved precipitation and enhanced updrafts. The model becomes more sensitive to the grid-scale updrafts than local thermodynamics at high rain rates as the contribution from the resolved precipitation increases. On the contrary, the observed tropical precipitation extremes do not show a strong sensitivity to the grid-scale updrafts.

Plain Language Summary

State of the art global scale climate models have horizontal resolutions of the order of tens of kilometers. However, these resolutions are much lower than the scales required to resolve tropical convection. This study investigates whether a resolution increase from 100 km to 25 km leads to any notable improvements in tropical rainfall simulation. Higher resolution simulations capture more intense rainfall events that are missed by their coarser counterparts. However, they struggle to capture the accurate frequency distribution of intense rainfall events. In addition, intense precipitation events in higher resolution simulations have different environmental conditions than the observed intense precipitation events. Results reported in this study underscore the importance of scrutinizing and carefully interpreting the outcomes of high-resolution climate model simulations.

1 Introduction

The representation of tropical rainfall is severely limited by the horizontal resolution of climate models, which is usually at the order of 100 km, whereas typical widths of upward motion in mature convective systems are in order of a few hundred meters to several kilometers (LeMone & Zipser, 1980; Matsuno, 2016). Convective systems interact with atmospheric circulation at various scales ranging from mesoscale to planetary-scale motions (Tomassini, 2020). Though many efforts have been made to count for the unresolved convection via the cumulus parameterization, these schemes are far from perfect and suffer large uncertainties. Therefore, increasing the resolution and improving cumulus parameterization remain the major focus areas of model development.

Though increasing horizontal resolution has model-dependent impacts, some common features are shared by a variety of general circulation models. They include increased contribution from the resolved precipitation, an intensified mean hydrological cycle and a higher frequency of precipitation extremes (Pope & Stratton, 2002; Demory et al., 2014; Hertwig et al., 2015; Terai et al., 2018; Herrington & Reed, 2020). Studies have also reported improved simulations of tropical and extratropical cyclones as the horizontal resolution increases (Zhao et al., 2009; Jung et al., 2012; Bacmeister et al., 2014; Demory et al., 2014). High-resolution ($\sim$50 km) versions of the Geophysical Fluid Dynamics Laboratory's (GFDL) gerneral circulation model have shown significant improvements in simulations of tropical cyclones, atmospheric rivers, mesoscale convective systems and precipitation extremes (Zhao et al., 2009; Murakami et al., 2020; Zhao, 2020, 2022; Dong et al., 2023; Jong et al., 2023).

Finer scales of resolved motions and a better representation of orography in high resolution simulations are recognized to improve the representation of precipitation extremes. Studies show that stronger vertical motions result in strengthening of precipitation (eg., Terai et al. (2018); Herrington and Reed (2020)). However, a recent study using aquaplanet simulations at resolutions ranging from 50 km to 6 km (Lin et al., 2022) show that increasing vertical motion do not fully explain the changes in precipitation intensity in high resolution simulations. Donner et al. (2016) highlight the need to assess the influence of vertical motions in examining the impacts of changing resolution and simulating convection in the models. Precipitation extremes over land, the global mean precipitation rates, their patterns and evaporation rate do not always show consistent improvement as the model resolution increases (Bador et al., 2020; Pope & Stratton, 2002; Hourdin et al., 2013; Bacmeister et al., 2014; Hertwig et al., 2015). Therefore, it is essential to develop a process-based understanding of how increasing resolution changes the simulation of rainfall. In the present work, we use GFDL's AM4 model to examine tropical rainfall distribution for three different resolutions viz., 100 km, 50 km and 25 km. We assess the frequency distribution of rainfall rates using the theoretical precipitation scaling diagnostic proposed by O'Gorman and Schneider (2009).

2 Data and methods

We use the GFDL atmospheric model version 4 (AM4) (Zhao et al., 2018a, 2018b) at three horizontal resolutions. The default GFDL AM4 utilizes a cubed-sphere topology for the atmospheric dynamical core with 96×96 grid boxes (c96) per cube face resulting in a horizontal resolution of ∼100 km. Here, we use two additional high resolution AM4 versions with 192×192 (c192) and 384×384 (c384) grid boxes per cube face, corresponding to horizontal resolutions of ∼50 km and ∼25 km, respectively. The default GFDL AM4.0 (Zhao et al., 2018a, 2018b) serves as the atmospheric component of GFDL's physical climate model (CM4, Held et al. (2019)), which participated in phase 6 of the Coupled Model Intercomparison Project (CMIP6, Eyring et al. (2016)). c192AM4 (Zhao, 2020) participated in the CMIP6 High Resolution Model Intercomparison Project (HighResMIP, Haarsma et al. (2016)). All three resolutions share the same atmospheric parameter setting as c192AM4 to remove uncertainties due to tuning. The parameter setting is documented in Zhao (2020). The default AM4 model's performance is reported in Zhao et al. (2018a) and Zhao et al. (2018b). The performance of c192AM4 in simulating the mean precipitation and precipitation extremes is documented in detail in Zhao (2020) and Zhao (2022).

The global mean precipitation in three different resolutions viz., c96, c192, and c384 are 2.92 $mm\ day^{-1}$, 2.96 $mm\ day^{-1}$, and 2.99$mm\ day^{-1}$, respectively for the period 1980-2000. The global mean precipitation increases progressively as the horizontal resolution of the model increases. Earlier studies (Duffy et al., 2003; Terai et al., 2018; Herrington & Reed, 2020) have noted a similar effect of horizontal resolution on simulated precipitation. These values are higher than the observed global mean precipitation of 2.67 $mm\ day^{-1}$ obtained using the the Global Precipitation Climatology Project (GPCP) dataset one degree daily dataset (1DD) Version 1.3 (Huffman et al., 2001) over the same period. Disagreement in the net longwave and shortwave fluxes at the surface (Supplementary Table 1) compared to observations (Trenberth et al., 2009) hint towards the differences in the mean simulated precipitation than the observed values. However, it is also important to note that the reliability of the GPCP dataset has been controversial (Gehne et al., 2016) and the radiative fluxes at the surface in the model lie within the range of different observational estimates (Trenberth et al., 2009; Stephens et al., 2012; Wild et al., 2015; L'Ecuyer et al., 2015). The excessive precipitation in the Western Pacific near the Philippines (also known as the "'Philippines hotspot" bias) and the dry biases over the eastern Atlantic and the Indian Ocean for c96 (Supplementary Fig. 1a) are reduced in c192 and c384 (Supplementary Fig. 1 b,c). However, the maritime continents (Supple-

mentary Fig. 1 b,c) and the eastern Pacific Inter Tropical Convergence Zone (ITCZ) move towards a wetter bias as the resolution increases. Tuning the model could improve some of the flux biases and thereby the mean precipitation biases. Zhao et al. (2018b) has investigated the effect of tuning on GFDL's AM4 precipitation in detail.

The model runs are analyzed for the historical period (1980-2000) at the daily frequency. We use daily precipitation dataset from the Tropical rainfall measurement mission (TRMM) version 3B42 (Huffman et al., 2007) and GPCP (Huffman et al., 2001) to compare the model performance with observations. The comparison of the model runs with observations are done for a common period of 1998-2000 over the tropics (30°S-30°N). In addition, we use the daily mean of the European Centre for Medium-Range Weather Forecasts (ECMWF) Reanalysis v5 (ERA5) (Hersbach et al., 2020) data at a horizontal resolution of $1^\circ \times 1^\circ$ for tropospheric temperature and winds. All model and observational variables are regridded to $1^\circ \times 1^\circ$ horizontal resolution using conservative remapping algorithm (python-cdo, (Schulzweida, 2022)). Histograms are normalized by a total number of data points that includes both rainy and non-rainy days.

3 Results

3.1 Rainfall intensity and frequency distribution

Figure 1 shows the normalized histogram of total daily precipitation intensity from the model at three resolutions (c96, c192, and c384) and observations (TRMM and GPCP). The normalized histogram (Fig. 1a) shows the most frequent nonzero rain rate. The simulated tropical rainfall peaks at ~ 1 $mm\ day^{-1}$. On the other hand, GPCP has a peak near $\sim$10-15 $mm\ day^{-1}$. All three resolutions produce more frequent rainfall than observations at lower rainrates (≤ 10 $mm\ day^{-1}$). This *too frequent too light* precipitation bias (also known as drizzle bias) is a shared problem in the most general circulation models (Sun et al., 2006; Wilcox & Donner, 2007; Stephens et al., 2010; Pendergrass & Hartmann, 2014). It is also important to note that the observations suffer from the underestimation of light rainfall (Behrangi et al., 2012). TRMM has a broad frequency distribution without any clear peak. Precipitation radar aboard TRMM has a minimum detectable signal of 17 dBz, making it poorly suited for detection of light rainfall (Behrangi et al., 2012; Kummerow et al., 1998). The discrepancy in the frequency of light rainfall is therefore partly attributed to the observational uncertainty.

The impact of horizontal resolution is evident at moderate rainfall rates. Interestingly, c384 has a notable reduction in the frequency near the secondary peak for c96 and c192 ($\sim 3-10$ $mm\ day^{-1}$). The bimodal frequency distribution of rainfall in c96 and c192 becomes monomodal in c384. The removal of a secondary peak in c384 is mainly due to the reduction in parameterized rainfall in c384 at these rainrates (Fig. 1c). All three resolutions produce less frequent rainfall at moderate rainfall rates ($20-40$ $mm\ day^{-1}$) compared to observations. On the contrary, the frequency of heavy rainfall ($\geq$ 100 $mm\ day^{-1}$) is overestimated compared to GPCP in all three resolutions. The frequency of high precipitation events in the model is closer to TRMM than GPCP. The retrieved precipitation in TRMM is shown to be more reliable than GPCP at higher rain rates (Behrangi et al., 2012). The frequency of heavy rainfall in c384 and c192 is overestimated compared to TRMM, whereas it is underestimated in c96.

The normalized histogram with a linear rainfall intensity scale (Fig. 1b) highlights the upper tail of rainfall distribution. The model produces progressively more frequent high rainfall events as the resolution increases. A few rare events with very high intensity (≥ 300 $mm\ day^{-1}$) are captured by c384 and c192 but not by c96. The observed precipitation tail goes up to 1000 $mm\ day^{-1}$, which is not captured by either resolution. On the contrary, it is also important to note that the frequency of high precipitation events ($\sim$200-400 $mm\ day^{-1}$) is overestimated in high resolution simulations (c192 and c384)

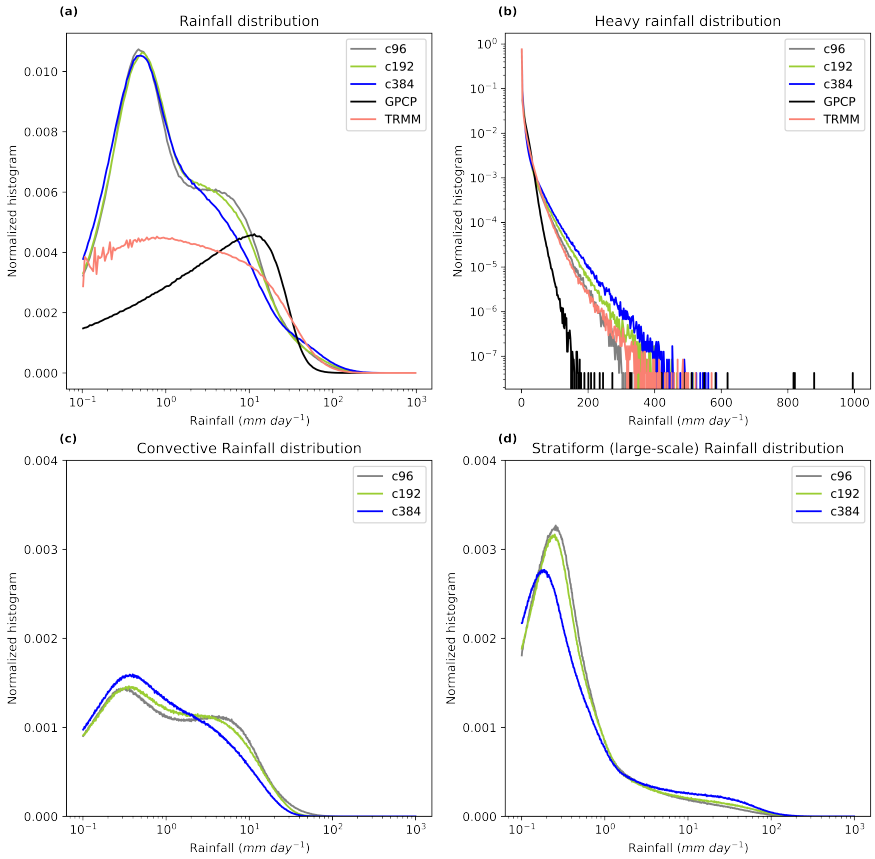

Figure 1. Normalized histogram of the daily mean rainfall (a) over logarithmic-scaled bins (rainfall intensity in $mm\ day^{-1}$), (b) over a linear-scaled bins (rainfall intensity) and a logarithmic scale for y-axis (normalized histogram) to highlight the upper end of the distribution. Normalized histogram for (c) convective rainfall, (d) resolved/large-scale rainfall. The simulated (c96, c192, c384) and observed (TRMM and GPCP) precipitation datasets are regridded to $1°\times1°$ horizontal resolution using conservative remapping algorithm. Histograms are normalized by a total count of datapoints considering both rainy and nonrainy days. The figure is plotted for an overlap period of 1998-2000 for the model runs and observations over the tropics (30°S-30°N).

compared to the observations. This analysis shows that the model produces intense tropical rainfall with the increasing horizontal resolution, but it overestimates the frequency of precipitation extremes.

3.2 Factors affecting the rainfall intensity distribution

Increasing the horizontal resolution changes the partitioning between precipitation produced by the convection scheme (parameterized precipitation, *prec_conv*) and the large-scale scheme (resolved precipitation, *prec_ls*). The contribution of resolved precipitation to the mean precipitation in the tropics increases from about 30% in c96 to more than 50% in c384 (Supplementary Fig. 2). The normalized frequency distribution for convective rainfall shifts towards lower intensity as the horizontal resolution increases (Fig. 1c). It is indicated by a progressively higher peak of normalized histogram at low convective

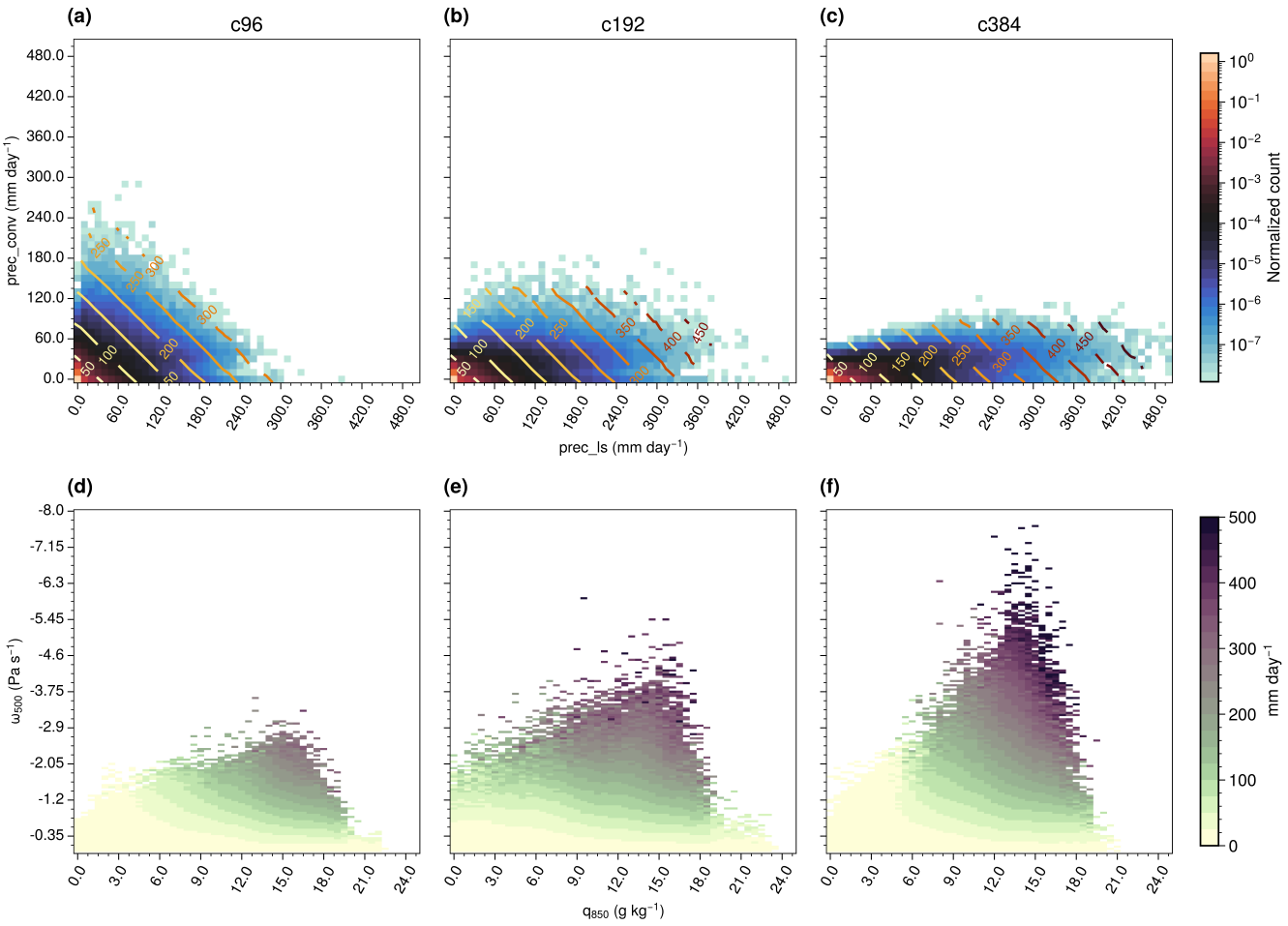

Figure 2. (a) 2D bin mean of normalized count (shading) and mean precipitation intensity (in $mm\ day^{-1}$ indicated by contours) as a function of convective (prec_conv) and large-scale (prec_ls) rainfall. (b) 2D bin mean precipitation intensity ($mm\ day^{-1}$) as a function of low-level moisture (q_{850}) and mid-tropospheric pressure velocity (ω_{500}). The figure is plotted for model simulations over a historical period of 1980-2000.

rainfall rates ($\leq$2 $mm\ day^{-1}$) and a reduction in the frequency at higher rainrates as the horizontal resolution increases (Fig. 1c). On the other hand, the frequency of large-scale rainfall exhibit a reduction in the peak at low rainfall rates and an increase at high rain rates for high resolution runs (Fig. 1d). This shows that the large-scale scheme progressively does more work at high rainfall intensities as the horizontal resolution increases. Figure 2 a-c shows the joint distribution of the resolved and the parameterized precipitation. The shading represents the 2D bin mean normalized count and the contours show the mean precipitation intensity. The count is normalized by a total number of datapoints considering both rainy and non-rainy days. For c96, both parameterized and large-scale schemes contribute almost equally at all precipitation intensities. However, the partitioning between parameterized and resolved precipitation changes in c192 and c384. Intense rainfall in c192 and c384 comes mainly from the large-scale scheme. Convective rainfall in c96 contributes up to a maximum intensity of 300 $mm\ day^{-1}$. However, it de-

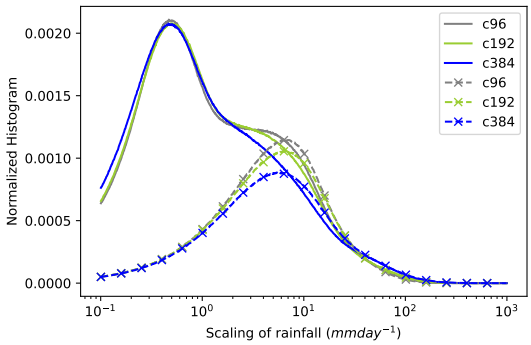

Figure 3. Normalized histogram of the model simulated mean daily rainfall (solid lines) and rainfall obtained from the theoretical precipitation scaling (marked-dotted lines) using equation (1). The histograms are plotted for the model runs over a historical period of 1980-2000.

creases below 200 $mm\ day^{-1}$ in c192 and it decreases even further in c384 (below 120 $mm\ day^{-1}$).

Two important ingredients to understand the rainfall intensity distribution are moisture and updraft velocity. We look at the 2D distribution of precipitation intensity as a function of low level moisture (q_{850}) and mid-tropospheric updraft velocity (ω_{500}) for three different resolutions (Fig. 2). As expected, rainfall intensity increases as moisture content and vertical velocity increase. The range of moisture content in three resolutions is not much different, however, the maximum vertical velocity increases by a factor of ~ 1.7 from c96 to c192, and about $\sim$2.3 from c96 to c384. Intense rainfall at finer resolutions mainly occurs at high updraft velocity (Fig. 2 e, f). In addition, the sensitivity of the precipitation intensity to high updraft velocity is contributed mainly by the resolved precipitation (Supplementary Fig. 3). In all three resolutions, large-scale precipitation shows a more sensitivity to updrafts than moisture (Supplementary Fig. 3 d-f). The parameterized precipitation instead shows sensitivity to low-level moisture unlike the resolved precipitation (Supplementary Fig. 3 a-c). Qualitative similarities between the total rainfall intensity distribution (Fig. 2 d-f) and the resolved precipitation (Supplementary Fig. 3 d-f) suggests that the sensitivity of precipitation intensity to the updraft velocity at high rainrates comes primarily from the resolved precipitation. This analysis indicates that as the horizontal resolution increases, the increase in rainfall intensity is associated primarily with the enhanced updraft velocity rather than the moisture content, and these changes come mainly from resolved (large-scale) precipitation.

3.3 Precipitation scaling

To further understand the impact of horizontal resolution on the rainfall frequency distribution, we use the precipitation scaling diagnostic proposed by O'Gorman and Schneider (2009). This diagnostic has been used primarily to study the changes in precipitation extremes with warming (O'Gorman, 2012; Singh & O'Gorman, 2014; Pfahl et al., 2017; Nie et al., 2018). The scaling is given by

$$P \approx -\left\{\omega \frac{\partial q_s}{\partial p}|_{\theta^*}\right\} \tag{1}$$

where precipitation intensity (P) is calculated from a column integrated product of pressure velocity (ω) and the vertical derivative of saturation specific humidity taken along a moist adiabat profile($\frac{\partial q_s}{\partial p}|_{\theta^*}$). The right hand side of the equation (1) corresponds to the column integrated condensation rate. The condensation maintains saturation of the

rising air parcel. This scaling assumes that precipitation efficiency is ~ 1 and all of the condensed water vapor falls as rainfall. The diabatic effects other than latent heating are neglected (θ^* is conserved; shown by Muller et al. (2011)). This scaling is expected to work better at higher precipitation intensities when air parcels are nearly saturated. However, we test it at all intensities.

The scaling captures the spatial distribution of deep convective areas of the tropics quite well, but it underestimates the intensity of the mean rainfall (Supplementary Fig. 4). Despite the assumptions mentioned earlier, the scaling captures the frequency distribution of rainfall at moderate to high intensity remarkably well in all three resolutions (Fig. 3 a). The scaling does not capture the model drizzle. We will discuss the possible reasons for it shortly. The frequency distribution of rainfall obtained by the scaling is monomodal. It peaks near 5-8 $mm\ day^{-1}$ for all three resolutions, which is close to the secondary peak of rainfall frequency distribution in c96 and c192. The scaling accurately produces this peak and captures the increasing magnitude from c384 to c96. After this peak, the precipitation scaling closely follows the frequency of simulated precipitation in all three resolutions. At moderate and high rainfall intensities, it overestimates the frequency of model simulated precipitation. However, the scaling captures the overall shape at high rain rates, including a peak in c384 near 50 $mm\ day^{-1}$.

As the contribution from radiative fluxes other than latent heat is non-negligible (θ^* is not conserved) at low rainfall intensity, the scaling is not expected to work at low rain rates. In addition, the model drizzle mainly comes from the subsaturated regions ($q \ll q_s$) (Terai et al., 2016). Earlier work suggests that a crude representation of parameterized convection could be the cause of drizzle bias in the models (Suzuki et al., 2013; Stephens et al., 2010). As we use grid-scale (resolved) variables to estimate the precipitation scaling, it can not capture subgrid scale convective processes. The above reasons possibly explain why precipitation scaling does not reproduce an accurate frequency of the model drizzle. In addition, the above scaling formulation does not include precipitation efficiency. The large-scale precipitation efficiency is affected by several factors such as mid level moisture, Convective available potential energy (CAPE), convective organization and microphysical processes (Muller & Takayabu, 2020; Zhao et al., 2016; Singh & O'Gorman, 2014). The overestimation of high rain rates by the scaling is likely due to the omission of precipitation efficiency in the calculations.

We plot the 2D bin mean of normalized precipitation intensity as a function of column-integrated vertical velocity ($\{\omega\}$) and the column-integrated vertical derivative of saturated specific humidity ($\left\{\frac{\partial q_s}{\partial p}|_{\theta*}\right\}$) (Fig. 4). As the maximum precipitation intensity in simulations and observations vary over a large range (Fig. 1 b), we normalize precipitation intensity by the maximum 2D bin mean value for each dataset. The precipitation intensity distribution without normalizing has similar features (Supplementary Fig. 5). The increase in precipitation intensity at higher resolution comes mainly from the changes in updraft velocity rather than changes in thermal stratification ($\left\{\frac{\partial q_s}{\partial p}|_{\theta*}\right\}$) as the horizontal resolution increases (Fig. 4 a-c). Intense precipitation events in the model are strongly tied to the grid-scale updrafts unlike observations (Fig. 4 e-f). We see that observed heavy precipitation events can occur even at moderate updrafts if the thermal stratification (Fig. 4 e-f, Supplementary Fig. 5 e-f) or low-level moisture (Supplementary Fig. 6 e-f) is high. Interestingly, ERA5 precipitation is also tied to stronger grid-scale updrafts but relatively to a lesser extent than GFDL's AM4 model. In c384, the grid-scale updrafts are much more intense than the reanalysis updrafts. The maximum grid-scale updraft at 500 hPa in c384 is about two times the maximum grid-scale updraft in ERA5 (Supplementary Fig. 6). It should be noted that the updrafts in reanalysis datasets suffer from uncertainties (Uma et al., 2021). Nonetheless, observational studies have noted the importance of local thermodynamics for tropical rainfall and the onset of precipitation (Houze Jr, 1989; Bretherton et al., 2004; Neelin et al., 2022). A typical size of updrafts in tropical convective systems is in order of a few kilometers (LeMone & Zipser,

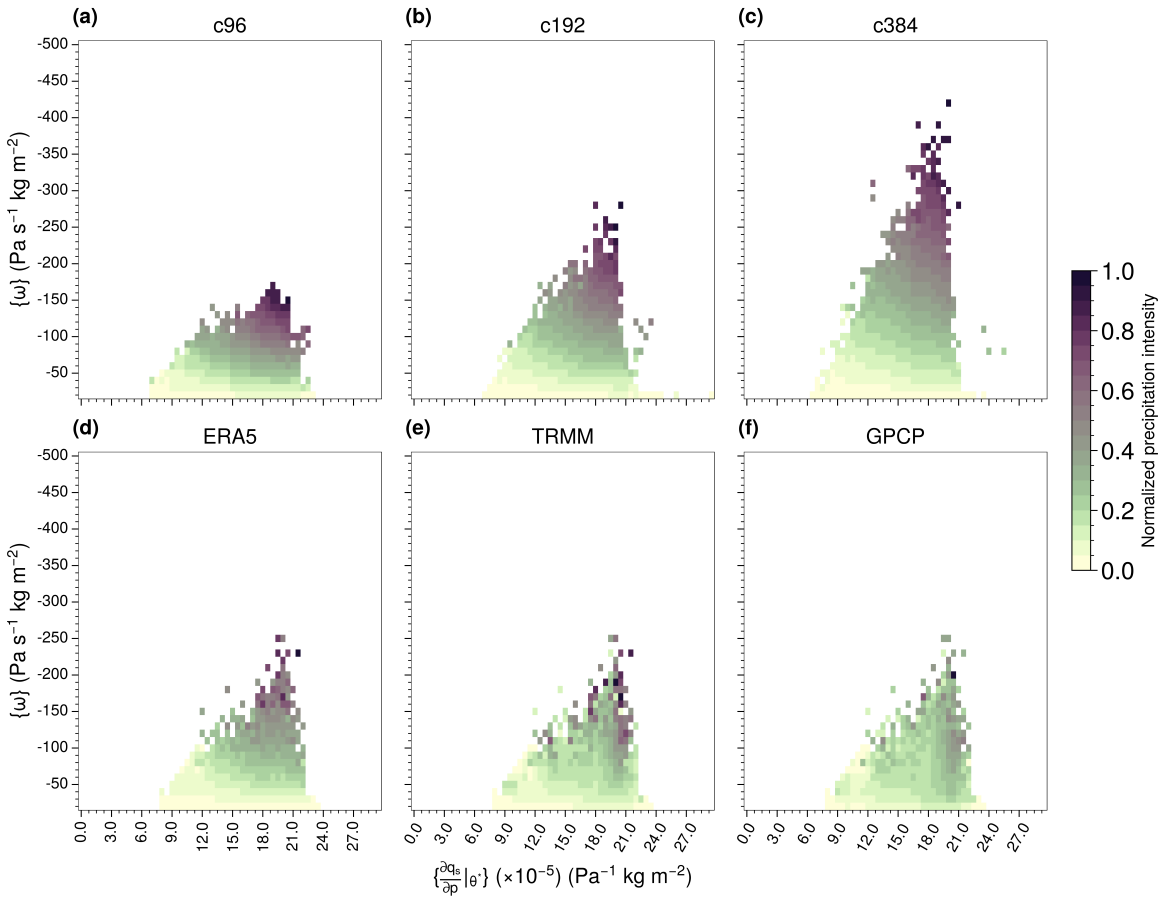

Figure 4. 2D bin mean of normalized precipitation intensity as a function of column-integrated pressure velocity $\{\omega\}$ and the column-integrated vertical derivative of saturated specific humidity along the moist adiabat $\left\{\frac{\partial q_s}{\partial p}|_{\theta*}\right\}$. Precipitation intensity (in $mm\ day^{-1}$) is normalized by maximum 2D bin value for each subplot. The figure is plotted using the data for an overlap period of 1998-2000.

1980; Matsuno, 2016), we would expect the cancellation of updrafts and downdrafts when averaged over an area of $\sim 1°\times1°$. In turn, we expect to see a less dependence of grid-scale updrafts for observed precipitation extremes.

Intense precipitation in c384 and c192 are closely tied to strong updrafts. The sensitivity of the simulated precipitation to the grid-scale updraft velocity mainly comes from the resolved precipitation and not from the parameterized precipitation (Supplementary Fig. 3). In this regard, tropical precipitation extremes in high resolution simulations exhibit similarities to grid-scale storms (Held et al., 2007). This suggests that even though the model is able to capture high intensity events as the horizontal resolution increases, with the increased contribution from the resolved precipitation, it comes at the expense of the model being overly sensitive to the grid-scale updraft velocity.

4 Discussion

We examine the distribution of tropical rainfall using GFDL's AM4 model at three horizontal resolutions viz., c96 (∼100 km), c192 (∼50 km) and c384 (∼25 km). As the horizontal resolution increases, we observe a progressive increase in the upper percentile of rainfall (precipitation extremes), increased contribution from the resolved precipitation and enhanced vertical velocities. These features are similar to earlier studies using different general circulation models (eg., Terai et al. (2018); Herrington and Reed (2020)). The model overestimates the frequency of light rainfall (drizzle bias) and underestimates the moderate rainfall in all three simulations. At finer resolutions (c192 and c384), the model produces more intense rainfall, but it overestimates the frequency of occurrence of heavy rainfall events compared to observed datasets (Fig. 1). The increase in precipitation extremes at high resolution is primarily contributed by the resolved precipitation and mainly comes from enhanced updrafts (Fig. 2).

We use theoretical precipitation scaling proposed by O'Gorman and Schneider (2009) to assess the frequency distribution of tropical rainfall. The scaling utilizes the grid-scale vertical velocity and temperature profiles to estimate an approximate precipitation intensity. Despite this simple formulation, the scaling produces the frequency distribution of model simulated precipitation remarkably well at moderate to high rain rates (Figure 3). Earlier studies have used the scaling to examine changes in precipitation extremes (O'Gorman, 2012; Singh & O'Gorman, 2014; Pfahl et al., 2017; Nie et al., 2018). In the GFDL model, the scaling reproduces the frequency distribution of tropical rainfall even at moderate rainfall rates ($\geq 10\ mm\ day^{-1}$). This could be a model dependent result, but it would be interesting to check the scaling for the other general circulation models.

Precipitation extremes in the model are closely tied to the grid-scale intense updrafts and relatively less sensitive to thermal stratification (Figure 4 a-c) and low-level moisture (Supplementary Fig. 6 a-c). In observed datasets, however, intense precipitation events can occur at moderate updraft velocities if thermal stratification (Figure 4 e-f) and low-level moisture are high (Supplementary Fig. 6 e-f). This high sensitivity of the model to updrafts comes mainly from the resolved precipitation (Supplementary Fig. 3). Convective precipitation shows sensitivity to local thermodynamics mimicking the observed tropical precipitation behavior closely (Bretherton et al., 2004; Neelin et al., 2022). On the other hand, resolved precipitation has been shown to capture geographical patterns and rain rates (Kooperman et al., 2018) better than parameterized precipitation. Convective precipitation also struggles to capture the accurate diurnal cycle of precipitation (Zhao et al., 2018a). This study suggests that the amount of rainfall obtained from the resolved precipitation and its sensitivity to the grid-scale vertical motion should be examined carefully atleast until the updrafts and downdrafts in convective systems are resolved explicitly. We reiterate the suggestion by Donner et al. (2016) on the importance of recognizing the dependence of resolved vertical velocity on resolution and utilizing it to understand the impacts of resolution realistically. Our results suggest that additional process-based evaluation is necessary to assess the performance of both parameterized and resolved precipitation.

References

Bacmeister, J. T., Wehner, M. F., Neale, R. B., Gettelman, A., Hannay, C., Lauritzen, P. H., ... Truesdale, J. E. (2014). Exploratory high-resolution climate simulations using the community atmosphere model (cam). *Journal of Climate*, *27*(9), 3073–3099.

Bador, M., Boé, J., Terray, L., Alexander, L. V., Baker, A., Bellucci, A., ... others (2020). Impact of higher spatial atmospheric resolution on precipitation extremes over land in global climate models. *Journal of Geophysical Research:*

Atmospheres, *125*(13), e2019JD032184.

Behrangi, A., Lebsock, M., Wong, S., & Lambrigtsen, B. (2012). On the quantification of oceanic rainfall using spaceborne sensors. *Journal of Geophysical Research: Atmospheres*, *117*(D20).

Bretherton, C. S., Peters, M. E., & Back, L. E. (2004). Relationships between water vapor path and precipitation over the tropical oceans. *Journal of climate*, *17*(7), 1517–1528.

Demory, M.-E., Vidale, P. L., Roberts, M. J., Berrisford, P., Strachan, J., Schiemann, R., & Mizielinski, M. S. (2014). The role of horizontal resolution in simulating drivers of the global hydrological cycle. *Climate dynamics*, *42*, 2201–2225.

Dong, W., Zhao, M., Ming, Y., Krasting, J. P., & Ramaswamy, V. (2023). Simulation of united states mesoscale convective systems using gfdl's new high-resolution general circulation model. *Journal of Climate*, 1–40.

Donner, L. J., O'Brien, T. A., Rieger, D., Vogel, B., & Cooke, W. F. (2016). Are atmospheric updrafts a key to unlocking climate forcing and sensitivity? *Atmospheric Chemistry and Physics*, *16*(20), 12983–12992.

Duffy, P., Govindasamy, B., Iorio, J., Milovich, J., Sperber, K., Taylor, K., ... Thompson, S. (2003). High-resolution simulations of global climate, part 1: present climate. *Climate Dynamics*, *21*, 371–390.

Eyring, V., Bony, S., Meehl, G. A., Senior, C. A., Stevens, B., Stouffer, R. J., & Taylor, K. E. (2016). Overview of the coupled model intercomparison project phase 6 (cmip6) experimental design and organization. *Geoscientific Model Development*, *9*(5), 1937–1958.

Gehne, M., Hamill, T. M., Kiladis, G. N., & Trenberth, K. E. (2016). Comparison of global precipitation estimates across a range of temporal and spatial scales. *Journal of Climate*, *29*(21), 7773–7795.

Haarsma, R. J., Roberts, M. J., Vidale, P. L., Senior, C. A., Bellucci, A., Bao, Q., ... others (2016). High resolution model intercomparison project (highresmip v1. 0) for cmip6. *Geoscientific Model Development*, *9*(11), 4185–4208.

Held, I. M., Guo, H., Adcroft, A., Dunne, J., Horowitz, L., Krasting, J., ... others (2019). Structure and performance of gfdl's cm4. 0 climate model. *Journal of Advances in Modeling Earth Systems*, *11*(11), 3691–3727.

Held, I. M., Zhao, M., & Wyman, B. (2007). Dynamic radiative–convective equilibria using gcm column physics. *Journal of the atmospheric sciences*, *64*(1), 228–238.

Herrington, A. R., & Reed, K. A. (2020). On resolution sensitivity in the community atmosphere model. *Quarterly Journal of the Royal Meteorological Society*, *146*(733), 3789–3807.

Hersbach, H., Bell, B., Berrisford, P., Hirahara, S., Horányi, A., Muñoz-Sabater, J., ... others (2020). The era5 global reanalysis. *Quarterly Journal of the Royal Meteorological Society*, *146*(730), 1999–2049.

Hertwig, E., von Storch, J.-S., Handorf, D., Dethloff, K., Fast, I., & Krismer, T. (2015). Effect of horizontal resolution on echam6-amip performance. *Climate Dynamics*, *45*, 185–211.

Hourdin, F., Foujols, M.-A., Codron, F., Guemas, V., Dufresne, J.-L., Bony, S., ... others (2013). Impact of the lmdz atmospheric grid configuration on the climate and sensitivity of the ipsl-cm5a coupled model. *Climate Dynamics*, *40*, 2167–2192.

Houze Jr, R. A. (1989). Observed structure of mesoscale convective systems and implications for large-scale heating. *Quarterly Journal of the Royal Meteorological Society*, *115*(487), 425–461.

Huffman, G. J., Adler, R. F., Morrissey, M. M., Bolvin, D. T., Curtis, S., Joyce, R., ... Susskind, J. (2001). Global precipitation at one-degree daily resolution from multisatellite observations. *Journal of hydrometeorology*, *2*(1), 36–50.

Huffman, G. J., Bolvin, D. T., Nelkin, E. J., Wolff, D. B., Adler, R. F., Gu, G., ... Stocker, E. F. (2007). The trmm multisatellite precipitation analysis (tmpa): Quasi-global, multiyear, combined-sensor precipitation estimates at fine scales. *Journal of hydrometeorology*, *8*(1), 38–55.

Jong, B.-T., Delworth, T. L., Cooke, W. F., Tseng, K.-C., & Murakami, H. (2023). Increases in extreme precipitation over the northeast united states using high-resolution climate model simulations. *npj Climate and Atmospheric Science*, *6*(1), 18.

Jung, T., Miller, M., Palmer, T., Towers, P., Wedi, N., Achuthavarier, D., ... others (2012). High-resolution global climate simulations with the ecmwf model in project athena: Experimental design, model climate, and seasonal forecast skill. *Journal of Climate*, *25*(9), 3155–3172.

Kooperman, G. J., Pritchard, M. S., O'Brien, T. A., & Timmermans, B. W. (2018). Rainfall from resolved rather than parameterized processes better represents the present-day and climate change response of moderate rates in the community atmosphere model. *Journal of advances in modeling earth systems*, *10*(4), 971–988.

Kummerow, C., Barnes, W., Kozu, T., Shiue, J., & Simpson, J. (1998). The tropical rainfall measuring mission (trmm) sensor package. *Journal of atmospheric and oceanic technology*, *15*(3), 809–817.

LeMone, M. A., & Zipser, E. J. (1980). Cumulonimbus vertical velocity events in gate. part i: Diameter, intensity and mass flux. *Journal of the Atmospheric Sciences*, *37*(11), 2444–2457.

Lin, P., Ming, Y., & Robinson, T. (2022). On the resolution sensitivity in a gfdl global atmospheric model. *Authorea Preprints*.

L'Ecuyer, T. S., Beaudoing, H., Rodell, M., Olson, W., Lin, B., Kato, S., ... others (2015). The observed state of the energy budget in the early twenty-first century. *Journal of Climate*, *28*(21), 8319–8346.

Matsuno, T. (2016). Prologue: tropical meteorology 1960–2010—personal recollections. *Meteorological Monographs*, *56*, vii–xv.

Muller, C., O'Gorman, P. A., & Back, L. E. (2011). Intensification of precipitation extremes with warming in a cloud-resolving model. *Journal of Climate*, *24*(11), 2784–2800.

Muller, C., & Takayabu, Y. (2020). Response of precipitation extremes to warming: what have we learned from theory and idealized cloud-resolving simulations, and what remains to be learned? *Environmental Research Letters*, *15*(3), 035001.

Murakami, H., Delworth, T. L., Cooke, W. F., Zhao, M., Xiang, B., & Hsu, P.-C. (2020). Detected climatic change in global distribution of tropical cyclones. *Proceedings of the National Academy of Sciences*, *117*(20), 10706–10714.

Neelin, J. D., Martinez-Villalobos, C., Stechmann, S. N., Ahmed, F., Chen, G., Norris, J. M., ... Lenderink, G. (2022). Precipitation extremes and water vapor: Relationships in current climate and implications for climate change. *Current Climate Change Reports*, *8*(1), 17–33.

Nie, J., Sobel, A. H., Shaevitz, D. A., & Wang, S. (2018). Dynamic amplification of extreme precipitation sensitivity. *Proceedings of the National Academy of Sciences*, *115*(38), 9467–9472.

Nikumbh, A., Lin, P., Paynter, D., & Ming, Y. (2023a, October). *Supporting data 1 for "Does increasing horizontal resolution improve the simulation of intense tropical rainfall?".* Zenodo. Retrieved from `https://doi.org/10.5281/zenodo.8433128` doi: 10.5281/zenodo.8433128

Nikumbh, A., Lin, P., Paynter, D., & Ming, Y. (2023b, October). *Supporting data 2 for "Does increasing horizontal resolution improve the simulation of intense tropical rainfall?".* Zenodo. Retrieved from `https://doi.org/10.5281/zenodo.8433235` doi: 10.5281/zenodo.8433235

Nikumbh, A., Lin, P., Paynter, D., & Ming, Y. (2023c, October). *Supporting data 3 for "Does increasing horizontal resolution improve the simulation of intense tropical rainfall?".* Zenodo. Retrieved from `https://doi.org/10.5281/zenodo.8433237` doi: 10.5281/zenodo.8433237

O'Gorman, P. A. (2012). Sensitivity of tropical precipitation extremes to climate change. *Nature Geoscience*, *5*(10), 697–700.

O'Gorman, P. A., & Schneider, T. (2009). Scaling of precipitation extremes over a wide range of climates simulated with an idealized gcm. *Journal of Climate*, *22*(21), 5676–5685.

Pendergrass, A. G., & Hartmann, D. L. (2014). Changes in the distribution of rain frequency and intensity in response to global warming. *Journal of Climate*, *27*(22), 8372–8383.

Pfahl, S., O'Gorman, P. A., & Fischer, E. M. (2017). Understanding the regional pattern of projected future changes in extreme precipitation. *Nature Climate Change*, *7*(6), 423–427.

Pope, V., & Stratton, R. (2002). The processes governing horizontal resolution sensitivity in a climate model. *Climate Dynamics*, *19*, 211–236.

Schulzweida, U. (2022, October). *Cdo user guide.* Zenodo. Retrieved from `https://doi.org/10.5281/zenodo.7112925` doi: 10.5281/zenodo.7112925

Singh, M. S., & O'Gorman, P. A. (2014). Influence of microphysics on the scaling of precipitation extremes with temperature. *Geophysical Research Letters*, *41*(16), 6037–6044.

Stephens, G. L., L'Ecuyer, T., Forbes, R., Gettelmen, A., Golaz, J.-C., Bodas-Salcedo, A., ... Haynes, J. (2010). Dreary state of precipitation in global models. *Journal of Geophysical Research: Atmospheres*, *115*(D24).

Stephens, G. L., Li, J., Wild, M., Clayson, C. A., Loeb, N., Kato, S., ... Andrews, T. (2012). An update on earth's energy balance in light of the latest global observations. *Nature Geoscience*, *5*(10), 691–696.

Sun, Y., Solomon, S., Dai, A., & Portmann, R. W. (2006). How often does it rain? *Journal of climate*, *19*(6), 916–934.

Suzuki, K., Golaz, J.-C., & Stephens, G. L. (2013). Evaluating cloud tuning in a climate model with satellite observations. *Geophysical Research Letters*, *40*(16), 4464–4468.

Terai, C. R., Caldwell, P., & Klein, S. A. (2016). Why do climate models drizzle too much and what impact does this have. In *Agu fall meeting abstracts* (Vol. 2016, pp. A53K–01).

Terai, C. R., Caldwell, P. M., Klein, S. A., Tang, Q., & Branstetter, M. L. (2018). The atmospheric hydrologic cycle in the acme v0. 3 model. *Climate Dynamics*, *50*(9-10), 3251–3279.

Tomassini, L. (2020). The interaction between moist convection and the atmospheric circulation in the tropics. *Bulletin of the American Meteorological Society*, *101*(8), E1378–E1396.

Trenberth, K. E., Fasullo, J. T., & Kiehl, J. (2009). Earth's global energy budget. *Bulletin of the american meteorological society*, *90*(3), 311–324.

Uma, K. N., Das, S. S., Ratnam, M. V., & Suneeth, K. V. (2021). Assessment of vertical air motion among reanalyses and qualitative comparison with very-high-frequency radar measurements over two tropical stations. *Atmospheric Chemistry and Physics*, *21*(3), 2083–2103.

Wilcox, E. M., & Donner, L. J. (2007). The frequency of extreme rain events in satellite rain-rate estimates and an atmospheric general circulation model. *Journal of Climate*, *20*(1), 53–69.

Wild, M., Folini, D., Hakuba, M. Z., Schär, C., Seneviratne, S. I., Kato, S., ... König-Langlo, G. (2015). The energy balance over land and oceans: an assessment based on direct observations and cmip5 climate models. *Climate Dynamics*, *44*, 3393–3429.

Zhao, M. (2020). Simulations of atmospheric rivers, their variability, and response to global warming using gfdl's new high-resolution general circulation model. *Journal of Climate*, *33*(23), 10287–10303.

Zhao, M. (2022). A study of ar-, ts-, and mcs-associated precipitation and extreme precipitation in present and warmer climates. *Journal of Climate*, *35*(2), 479–497.

Zhao, M., Golaz, J.-C., Held, I., Guo, H., Balaji, V., Benson, R., ... others (2018a). The gfdl global atmosphere and land model am4. 0/lm4. 0: 1. simulation characteristics with prescribed ssts. *Journal of Advances in Modeling Earth Systems*, *10*(3), 691–734.

Zhao, M., Golaz, J.-C., Held, I., Guo, H., Balaji, V., Benson, R., ... others (2018b). The gfdl global atmosphere and land model am4. 0/lm4. 0: 2. model description, sensitivity studies, and tuning strategies. *Journal of Advances in Modeling Earth Systems*, *10*(3), 735–769.

Zhao, M., Golaz, J.-C., Held, I. M., Ramaswamy, V., Lin, S.-J., Ming, Y., ... others (2016). Uncertainty in model climate sensitivity traced to representations of cumulus precipitation microphysics. *Journal of Climate*, *29*(2), 543–560.

Zhao, M., Held, I. M., Lin, S.-J., & Vecchi, G. A. (2009). Simulations of global hurricane climatology, interannual variability, and response to global warming using a 50-km resolution gcm. *Journal of Climate*, *22*(24), 6653–6678.

Open Research Section

The AM4 model code is provided at `https://data1.gfdl.noaa.gov/nomads/forms/am4.0/` (Zhao et al., 2018a, 2018b). The configuration of the simulations presented in this manuscript is described in Zhao (2020). The model outputs used are available at: `https://zenodo.org/record/8433128`, `https://zenodo.org/record/8433235` and `https://zenodo.org/record/8433237` (Nikumbh et al., 2023a, 2023b, 2023c). The ERA5 data can be downloaded from `https://cds.climate.copernicus.eu/cdsapp#!/dataset/reanalysis-era5-complete?tab=overview` (Hersbach et al., 2020). The GPCP precipitation dataset is available `https://rda.ucar.edu/datasets/ds728.7/dataaccess/` (Huffman et al., 2001). The TRMM precipitation data is downloaded from `https://disc.gsfc.nasa.gov/datasets?keywords=TRMM_3B42_7&page=1` (Huffman et al., 2007).

Acknowledgments

A.C.N. acknowledges support from Cooperative Institute for Modeling the Earth System, AOS, Princeton University, and Geophysical Fluid Dynamics Laboratory (GFDL), NOAA. The initial version of the manuscript greatly benefited from discussions and inputs from Dr. Leo Donner and Dr. Bor-Ting Jong. We thank Dr. Yi-Huang Kuo and Dr. Issac Held for discussions, Dr. Ming Zhao, Dr. Wenhao Dong and Dr. Huan Gao for helping to set up the initial model runs. This work was done by A.C.N. under Award NA18OAR4320123 from the National Oceanic and Atmospheric Administration, U.S. Department of Commerce. The statements, findings, conclusions, and recommendations are those of the author(s) and do not necessarily reflect the views of the National Oceanic and Atmospheric Administration or the U.S. Department of Commerce.

Supporting Information for "Does increasing horizontal resolution improve the simulation of intense tropical rainfall?"

Akshaya C. Nikumbh[1,2], Pu Lin[1,2], David Paynter [2], Yi Ming[3]

[1] Atmospheric and Oceanic Sciences, Princeton University, Princeton, New Jersey

[2]Geophysical Fluid Dynamics Laboratory (NOAA), Princeton, New Jersey

[3]Schiller Institute for Integrated Science and Society, Boston College, Massachusetts

Contents of this file

1. Figures S1 to S6

2. Table S1

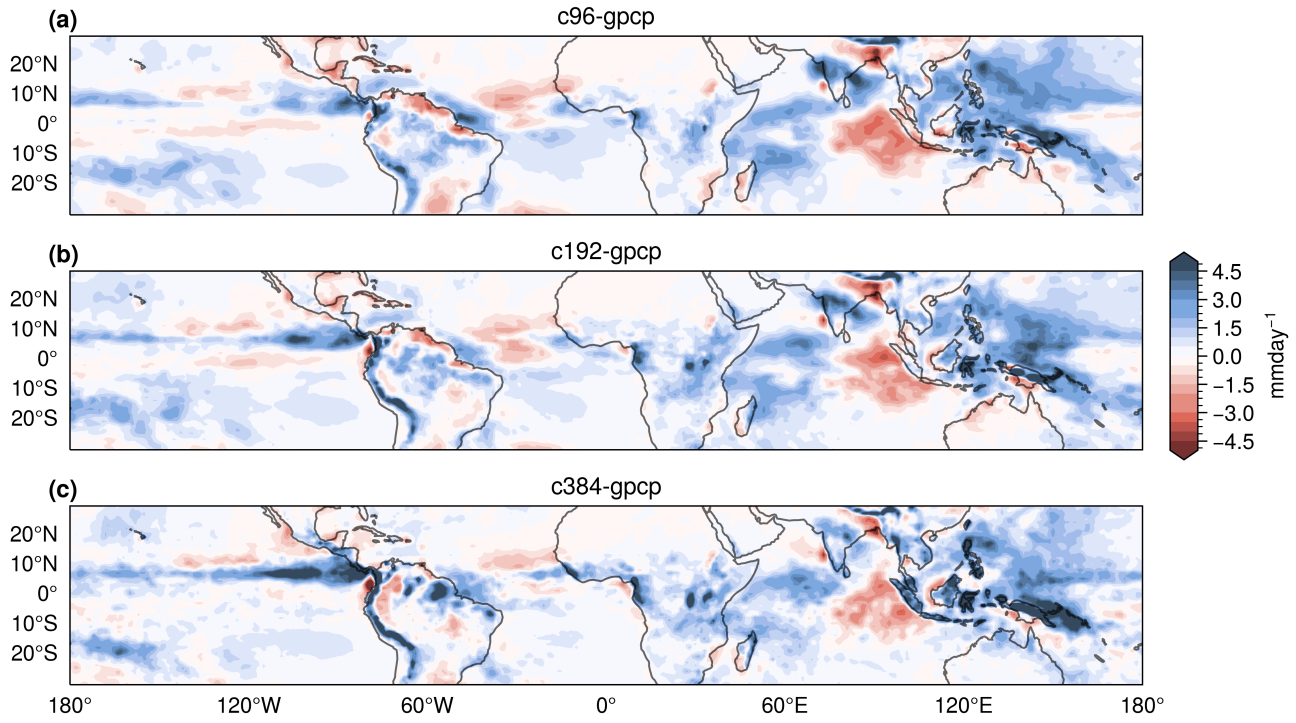

Figure S1. The difference in the mean rainfall between (a) c96 , (b) c192, and (c) c384 and the mean GPCP rainfall averaged over a period of 1998-2000.

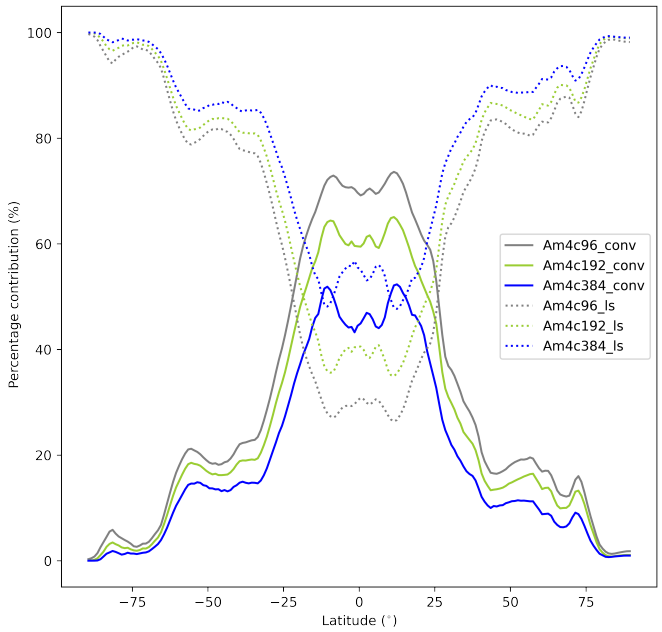

Figure S2. Percentage contribution by convective (solid) and large-scale rainfall (dotted lines) to zonally averaged mean rainfall for c96 (grey), c192 (green) and c384 (blue), respectively. The figure is obtained from the model runs over a period of 1980-2000.

Table S1. Global mean values for rainfall and terms in the radiation budget for the model runs over the period of 1980-2000. The values in blue indicate an increase with respect to c96 and red indicates the decrease. The statistically insignifacant change with respect to c96 ($pvalue \geq 0.05$ using student's t-test) is indicated by an asterisk (*) .

	c96	c192	c384
Net rainfall	2.92	2.96	2.99
Net TOA	2.14	1.79	2.29
SWUP_sfc	23.95	24.33	25.22
SWDN_sfc	187.80	189.28	192.06
LW_up_sfc	398.61	398.20	397.93
LW_dn_sfc	340.10	339.47	338.23
latent_sfc	84.51	85.70	86.55
sensible_sfc	17.93	17.96*	17.47

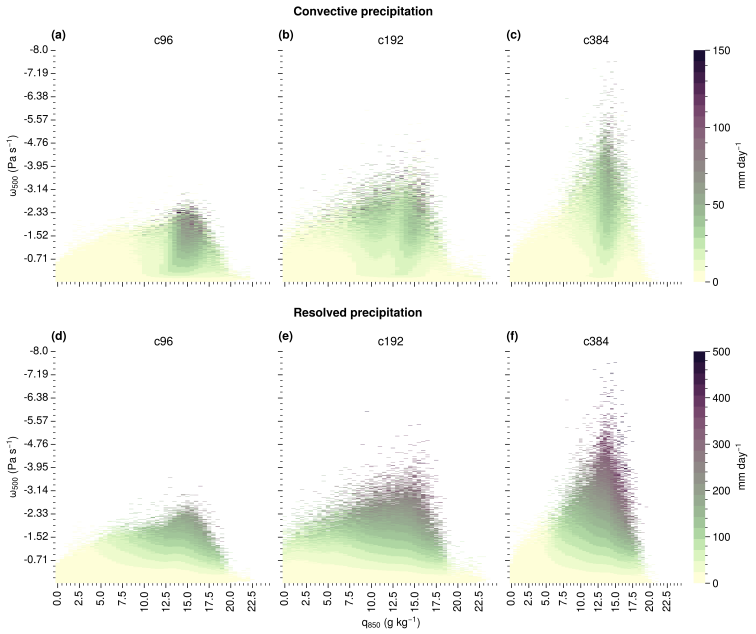

Figure S3. 2D bin mean convective and resolved precipitation intensity (in $mm\ day^{-1}$) as a function of midlevel vertical velocity (ω_{500}) and low-level moisture (q_{850}). The figure is obtained from the model simulations over a period of 1980-2000.

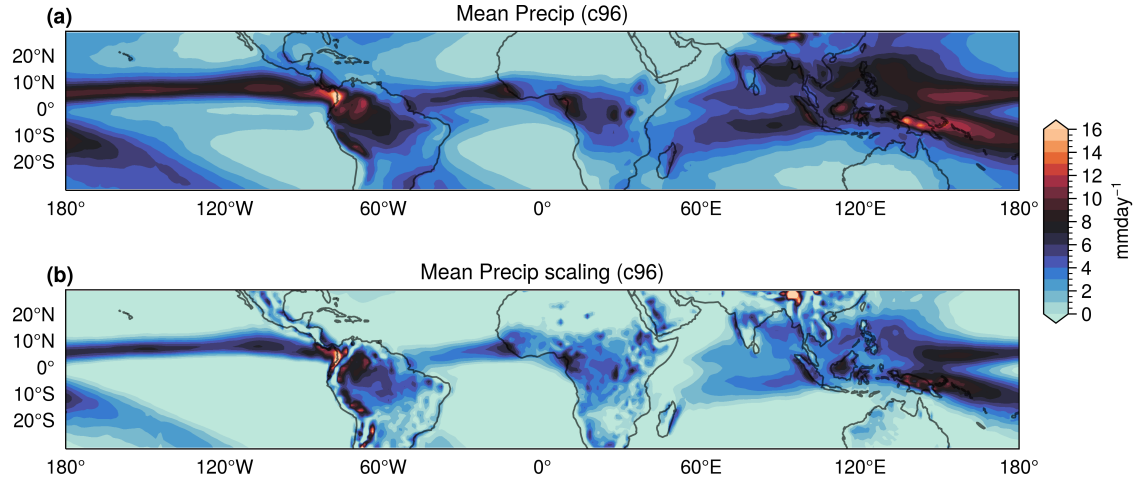

Figure S4. (a) Climatological daily mean precipitation intensity (in $mm\ day^{-1}$) in c96 (b) the mean rainfall intensity ($mm\ day^{-1}$) obtained from the precipitation scaling using equation (1). The figure is obtained from the model simulations over a period of 1980-2000.

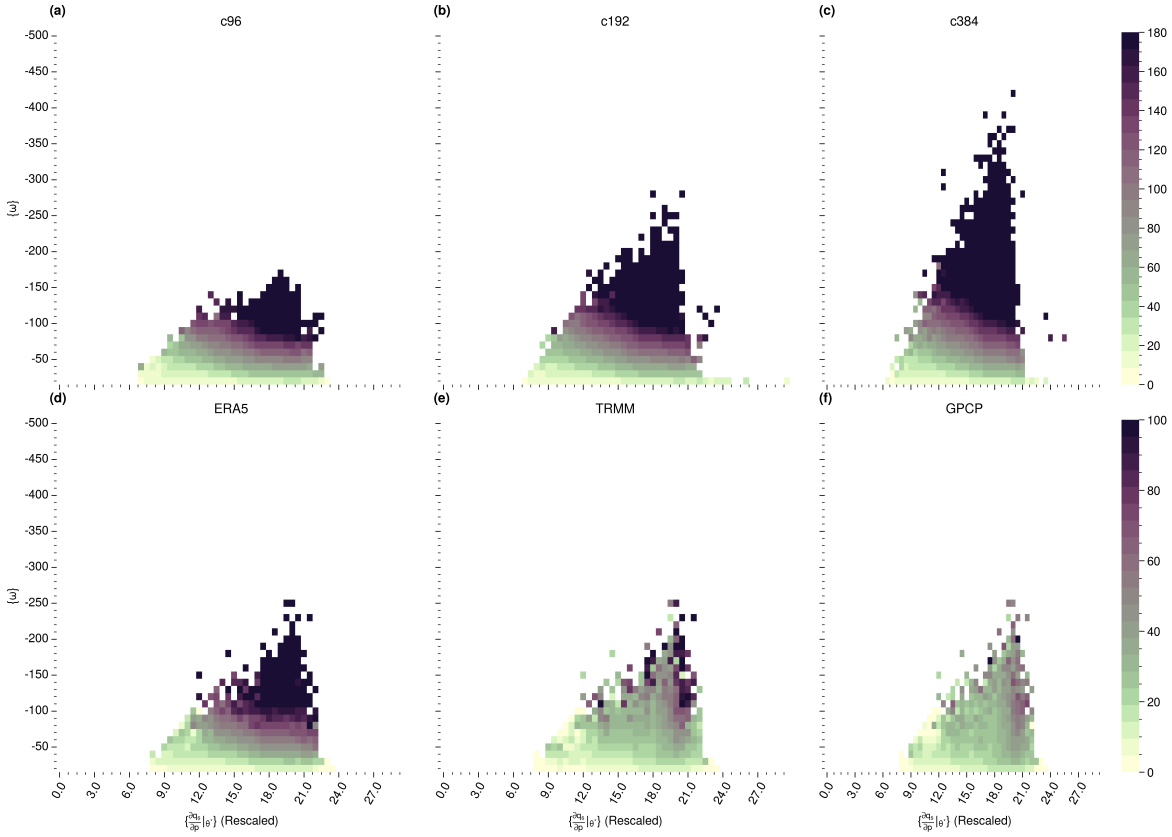

Figure S5. 2D bin mean of normalized precipitation intensity ($mm\ day^{-1}$) as a function of column-integrated pressure velocity $\{\omega\}$ and the column-integrated vertical derivative of saturated specific humidity along the moist adiabat $\left\{\frac{\partial q_s}{\partial p}|_{\theta*}\right\}$. The x-axis is scaled by a constant multiplier of 10^5. The figure is plotted using the data for an overlap period of 1998-2000.

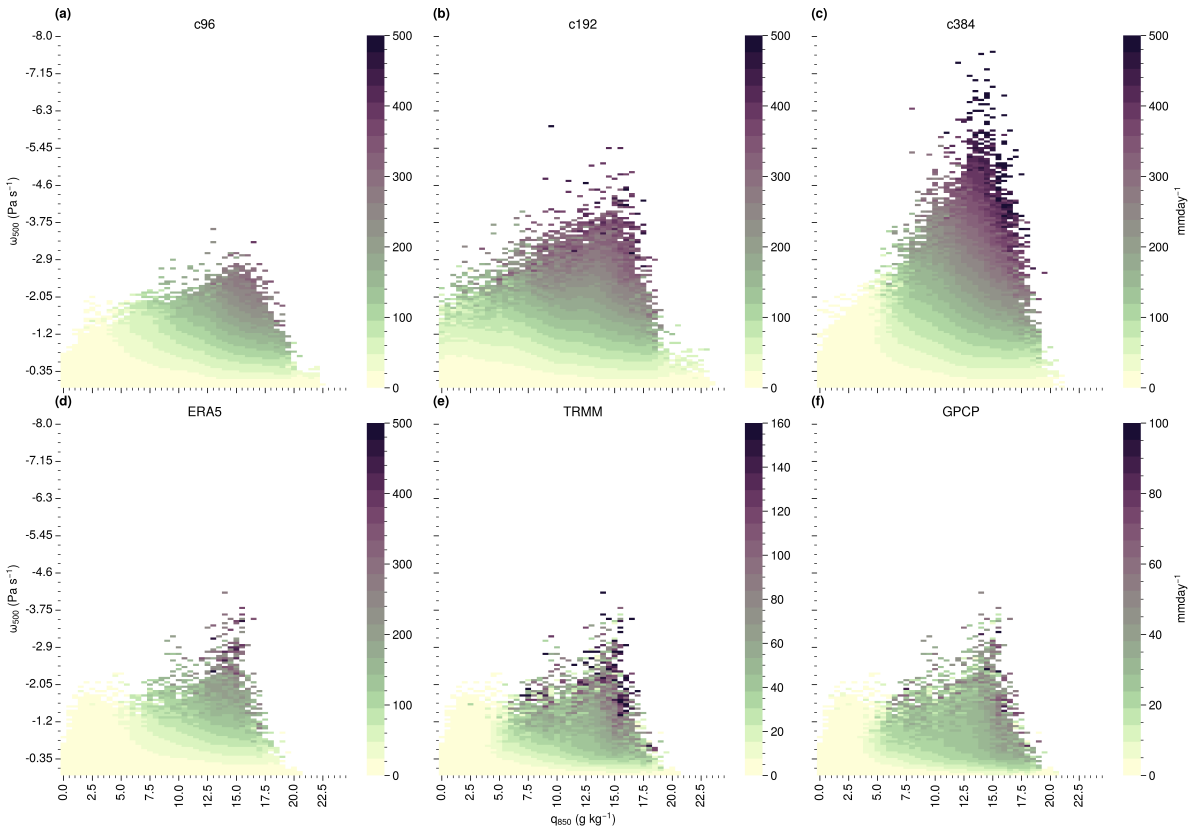

Figure S6. 2D bin mean of normalized precipitation intensity as a function of low-level moisture (q_{850}) and midtropospheric pressure velocity (ω_{500}). The figure is plotted using the data for an overlap period of 1998-2000.